Geophys. J. Int. (2005) **161,** 566–590 doi: 10.1111/j.1365-246X.2005.02625.x

The relationship between the spectral function and the underlying conductivity structure in 1-D magnetotellurics

Peter Weidelt

Institut für Geophysik und Extraterrestrische Physik, Technische Universität Braunschweig, D-38106 *Braunschweig, Germany. E-mail: p.weidelt@tu-bs.de*

Accepted 2005 February 28. Received 2005 February 25; in original form 2004 June 9

SUMMARY

The frequency response $c(\omega)$ in 1-D magnetotellurics admits a well-known integral representation with kernel $1/(\lambda + i\omega)$ and non-negative spectral function $w(\lambda)$, $\lambda \geq 0$. The purpose of this paper is to elucidate the hidden, but fundamental relationship between $w(\lambda)$ and the underlying conductivity structure $\sigma(z)$. The most important criterion for classifying the conductivity structure is the existence of moments of $w(\lambda)$: if all moments exist, $\sigma(z)$ consists of a finite or infinite number of thin sheets; the sheet parameters are obtained from orthogonal polynomials associated with the weight function $w(\lambda)$. If no moment (or only a finite number of moments) exists, $\sigma(z)$ contains sections with a piecewise continuous conductivity structure, possibly covered by thin sheets. In both cases, the spectrum may be continuous, completely discrete or a mixture of both. The great variety of possible spectral functions is illustrated by a plethora of examples. The present investigation has no immediate impact on practical inversion because the unstable determination of $w(\lambda)$ is mostly circumvented in the inversion of experimental data. Therefore, the rich morphology of the spectral function generally has escaped our attention.

Key words: electrical conductivity, electromagnetic induction, inverse theory, magnetotellurics.

1 INTRODUCTION

Because of its great simplicity, the inverse problem of 1-D magnetotellurics is the best studied inverse problem in geoelectromagnetism. An answer can be given to all relevant questions of uniqueness (Tikhonov 1965), existence (Weidelt 1986; Yee & Paulson 1988b) and construction (Parker 1980; Parker & Whaler 1981) of a solution. In particular, the last two issues are treated for incomplete data sets.

In the 1-D magnetotelluric problem, all field quantities depend on the depth coordinate z only, z positive downwards. The one-component electric and magnetic field vectors $\mathbf{E} = E\hat{\mathbf{x}}$ and $\mathbf{H} = H\hat{\mathbf{y}}$ satisfy for a time factor $\exp(i\omega t)$ the equations, using throughout the abbreviation $\zeta := i\omega$,

$$E'(z,\zeta) = -\zeta\mu_0 H(z,\zeta), \quad H'(z,\zeta) = -\sigma(z)E(z,\zeta), \tag{1.1}$$

where the prime denotes differentiation with respect to z and $\sigma(z) \geq 0$ is the electrical conductivity. Eliminating H from eq. (1.1) yields the ordinary differential equation

$$E''(z,\zeta) = \zeta\mu_0\sigma(z)E(z,\zeta). \tag{1.2}$$

If $E(z,\zeta)$ is the solution of eq. (1.2) with $E'(z,\zeta) \to 0$ for $z \to \infty$, then the magnetotelluric response function $c(\zeta)$, as defined by Schmucker (1970), is

$$c(\zeta) := \frac{E(0,\zeta)}{\zeta\mu_0 H(0^-,\zeta)} = -\frac{E(0,\zeta)}{E'(0^-,\zeta)}, \tag{1.3}$$

where provision is made for the case that, as a result of the presence of a thin conducting sheet, $H(z)$ may be discontinuous at the surface $z = 0$. The complex response function $c(\zeta)$ has the dimension of a length and admits the spectral representation (Weidelt 1972; Parker 1980; Yee & Paulson 1988a)

$$c(\zeta) = w_0 + \int_{0^-}^{\infty} \frac{w(\lambda)\,d\lambda}{\lambda + \zeta}, \quad w_0 \geq 0, \quad w(\lambda) \geq 0. \tag{1.4}$$

The constant w_0 in eq. (1.4) is the thickness of an insulating surface layer, below which the first conductor occurs. For simplicity, it is assumed that $w_0 = 0$, but a positive w_0 is easily introduced whenever required. The non-negative real function $w(\lambda)$ has to be considered as a generalized function to include both the continuous and discrete part of the spectrum. We avoid the more appropriate Stieltjes integral

notation and represent the discontinuous part by a superposition of δ-functions. Although the name 'spectral function' is usually reserved for $\int w(\lambda)\,d\lambda$, we shall apply it for simplicity also to $w(\lambda)$. The points $\lambda \geq 0$ with $w(\lambda) > 0$ correspond to the decay constants of freely decaying current systems $E(z, t) = e(z, \lambda)\exp(-\lambda t)$, defined by the eigenvalue problem

$$e''(z, \lambda) + \lambda\mu_0\sigma(z)e(z, \lambda) = 0, \quad e'(0^-, \lambda) = 0, \quad e(z, \lambda) \quad \text{finite for} \quad z \to \infty. \tag{1.5}$$

Using for the orthogonal modes the normalization

$$\int_{0^-}^{\infty} \mu_0\sigma(z)e(z, \lambda)e(z, \lambda')\,dz = \delta(\lambda - \lambda'), \tag{1.6}$$

the formal expansion of the solution of eq. (1.2) in terms of the eigenmodes is

$$E(z, \zeta) = -E'(0^-, \zeta)\int_{0^-}^{\infty} \frac{e(0, \lambda)e(z, \lambda)\,d\lambda}{\lambda + \zeta}, \tag{1.7}$$

yielding in view of eqs (1.3) and (1.4)

$$w(\lambda) = e^2(0, \lambda). \tag{1.8}$$

On the semi-axis $\zeta \leq 0$, a pole of $c(\zeta)$ at $\zeta = -\lambda_m$ with residuum w_m corresponds to a spectral line at $\lambda = \lambda_m$ with strength w_m and is represented in the spectral function by $w_m\delta(\lambda - \lambda_m)$. The lower limit 0^- in eq. (1.4) guarantees that a possible term $\sim\delta(\lambda)$ is fully included in the range of integration. A branch cut of $c(\zeta)$ in $\zeta < 0$ corresponds to a continuous section of the spectrum. In general, a mixture of spectral lines and (several) continuous sections occurs.

The best-studied spectrum consists of a finite number of discrete lines and is given by the typical spectral function

$$w(\lambda) = \sum_{m=1}^{N} w_m\delta(\lambda - \lambda_m) \quad \text{with} \quad w_m > 0, \lambda_m > 0 \tag{1.9}$$

with pairwise different λ_m. The $2N$ positive parameters of $w(\lambda)$ are mapped onto the $2N$ free positive parameters of the conductivity distribution

$$\sigma(z) = \tau_0\delta(z) + \sum_{n=1}^{N} \tau_n\delta(z - z_n) \quad \text{with} \quad z_n > 0, \tau_n > 0, \tau_N = \infty. \tag{1.10}$$

This conductor consists of a thin surface sheet with conductance (= depth integrated conductivity) τ_0, followed by N sheets with conductances τ_n at depths z_n. The terminating sheet is perfectly conducting. This degenerate class of conductivity models has to be considered when constructing in a D^+ interpretation of experimental magnetotelluric data the best-fitting 1-D model (Parker 1980; Parker & Whaler 1981).

Experimental data are collected on the imaginary ζ-axis (= real ω-axis), whereas the spectral function is associated with the behaviour of $c(\zeta)$ on the negative-real semi-axis,

$$w(\lambda) = -\frac{1}{\pi}\lim_{\epsilon \to 0^+} \Im c(-\lambda + i\epsilon), \tag{1.11}$$

where $\Im$ denotes the imaginary part (*cf.* Yee & Paulson 1988a, p. 272). This involves an unstable analytic continuation in the direction of the sources (*cf.* Fig. 1). Therefore, small details of the spectrum cannot be reliably inferred from experimental data and a representation of experimental data by approximating eq. (1.4) by a finite set of discrete lines,

$$c(\zeta) = w_0 + \sum_{m=1}^{N} \frac{w_m}{\lambda_m + \zeta}, \quad \lambda_m \geq 0, \quad w_m \geq 0, \tag{1.12}$$

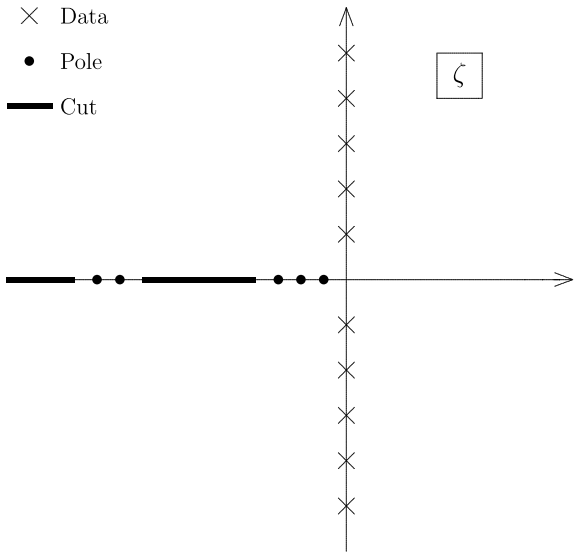

Figure 1. Response function $c(\zeta)$: Position of singularities and data in the complex ζ-plane.

will mostly be fully adequate. In theory, however, the spectrum is much richer: besides a finite number of discrete lines, it may consist of an infinite number of discrete lines or of one or several continuous sections, possibly with interlacing discrete lines. The aim of the present paper is to explore in some detail the relationship between the fine structure of the spectral function and the underlying 1-D conductivity structure. Although this study will be of limited relevance for the actual solution of the inverse problem, it visualizes a fundamental facet of the inverse problem, which generally escapes our attention.

Let the moment of order k of $w(\lambda)$ be defined as

$$s_k := \int_{0^-}^{\infty} w(\lambda)\lambda^k d\lambda, \quad k = 0, 1, 2, \ldots. \tag{1.13}$$

With regard to the existence of moments, two different classes of conductivity distributions have to be distinguished, as follows.

(i) If moments s_k of all orders k exist, then the underlying conductivity structure $\sigma(z)$ consists of a finite or infinite set of thin conducting sheets. The existence of all moments requires that $w(\lambda)$ is integrable and that either $w(\lambda) = 0$ for $\lambda > b$ (with $b < \infty$) or that $w(\lambda)$ decays very fast for $\lambda \to \infty$ (e.g. exponentially). The spectrum may be discrete or continuous or a mixture of both. This class is typically represented by the discrete spectrum (1.9) with the thin sheet structure (1.10).

(ii) If $w(\lambda)$ is not integrable at all or if only a finite number of moments s_k exists, then $\sigma(z)$ contains a piecewise continuous conductivity section, possibly lying under a finite number of thin sheets. To this class belong the spectral functions $w(\lambda)$ with a slow decay for $\lambda \to \infty$. (The integral representation (1.4) exists if the decay is as slow as $1/\lambda^{\epsilon}$, $\epsilon > 0$.) Again, the nature of the spectrum is arbitrary. A prominent representative of this class is the uniform half-space (conductivity σ_0), where

$$w(\lambda) = \frac{1}{\pi\sqrt{\lambda\mu_0\sigma_0}}. \tag{1.14}$$

For the thin-sheet models (i), we can develop a fairly complete theory, which is based on continued fractions (CFs) and orthogonal polynomials, well-studied mathematical subjects of the late 19th and early 20th century. Although the underlying theory of these subjects is well presented in text books (e.g. Perron 1913; Wall 1948; Szegö 1975), for a more self-contained treatment and a unified notation, some of the relevant material will be readdressed. A less complete theory can be formulated for the piecewise continuous conductivity models (ii). Here, the treatment will be limited to illustrative examples only.

The thin-sheet models (i) are studied in detail in Section 2 by representing the thin-sheet parameters both in terms of the orthogonal polynomials associated with the weight function $w(\lambda)$ and in terms of the moments s_k of $w(\lambda)$. The first formulation gives rise to a simple new numerical algorithm for calculating the sheet parameters from the spectral function. For illustration, the sequences of thin sheets derived from the classical orthogonal polynomials are treated in some detail.

Section 3 is devoted to the spectral functions of piecewise continuous conductivity structures, illustrated by means of simple examples. The appendices complement the material presented in the main part of the paper. In particular, Appendix B sketches the solution of the simplest forward problem, i.e. the determination of $w(\lambda)$ for a finite set of thin sheets.

2 THIN-SHEET CONDUCTIVITY STRUCTURES

2.1 Expression of the sheet parameters in terms of orthogonal polynomials

In this section, it is assumed that all moments s_k of the spectral function $w(\lambda)$ exist, i.e.

$$s_k := \int_{0^-}^{\infty} w(\lambda)\lambda^k d\lambda < \infty, \quad k = 0, 1, 2, \ldots. \tag{2.1}$$

The non-negative spectral function $w(\lambda)$ is interpreted as the weight function determining the scalar product of two functions $f(\lambda)$ and $g(\lambda)$,

$$(f, g) := \int_{0^-}^{\infty} w(\lambda) f(\lambda) g(\lambda)\, d\lambda, \tag{2.2}$$

where $f(\lambda)$ and $g(\lambda)$ are real-valued functions of the class $L^2_w(0, \infty)$. The existence of all moments allows the construction of a set of orthogonal polynomials $p_n(\lambda)$ of degree n, $n = 0, 1, 2, \ldots$, such that

$$(p_m, p_n) = h_n \delta_{mn}, \tag{2.3}$$

where δ_{mn} is the Kronecker symbol and h_n is the $L^2_w(0, \infty)$ norm of $p_n(\lambda)$. For $w(\lambda)$ consisting of a finite number of N discrete lines, the polynomials can be constructed only up to degree $N - 1$. However, if $w(\lambda)$ contains a continuous section, the orthogonal polynomials exist to an arbitrarily high degree. For instance, $w(\lambda) = s_0/(b - a)$ in $0 \le a \le \lambda \le b$, with $b > a$ and $w(\lambda) = 0$ elsewhere, is associated with the shifted Legendre polynomials

$$p_n(\lambda) = P_n\left(\frac{2\lambda - a - b}{b - a}\right), a \le \lambda \le b, n = 0, 1, 2, \ldots. \tag{2.4}$$

The polynomials are uniquely determined up to an amplitude factor at our disposal. Let this factor be the coefficient $k_n \neq 0$ of the leading power λ^n. Then the following result is proved.

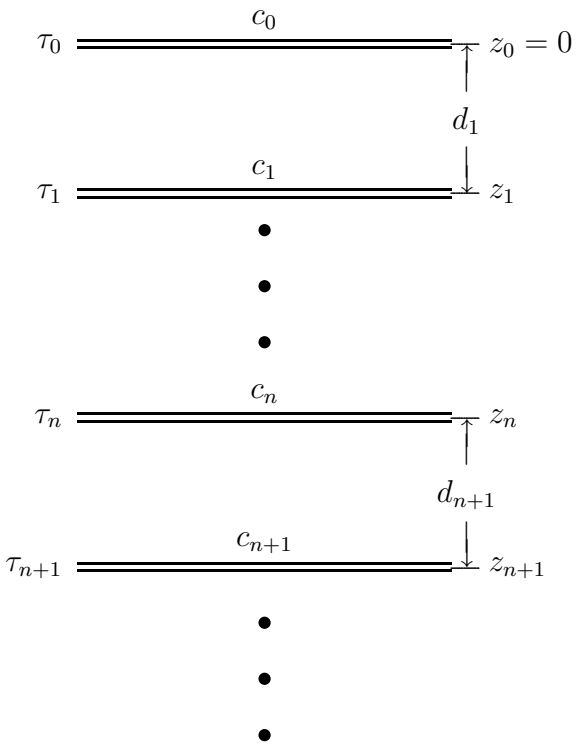

Figure 2. Thin-sheet model with conductances τ_n and intersheet separations d_n. The responses c_n, with $c_0 = c(\zeta)$ as the MT response, refer to the position z_n^- immediately above the sheet.

If all moments s_k of $w(\lambda)$ exist, the response function $c(\zeta)$ has to be interpreted by a stack of thin sheets with conductances τ_n and intersheet separations d_n (*cf.* Fig. 2), which can be expressed in terms of the orthogonal polynomials, evaluated at $\lambda = 0$, as

$$\mu_0 \tau_n = p_n^2(0)/h_n, n \geq 0, \tag{2.5}$$

$$d_{n+1} = -\frac{k_{n+1} h_n}{k_n p_n(0) p_{n+1}(0)}, n \geq 0. \tag{2.6}$$

If and only if $w(\lambda)$ is represented by a finite number of discrete lines [as in eq. (1.9)], is the number of sheets finite. So far no standardization (e.g. $h_n = 1$ or $k_n = 1$) of the polynomials $p_n(\lambda)$ has been applied, and the two dependent parameters k_n and h_n have been retained for flexibility. A simple numerical algorithm for the computation of the sheet parameters associated with a given weight function $w(\lambda)$ is presented in Section 2.2.

For a justification of the above result, it is first noted that the orthogonal polynomials $p_n(\lambda)$ satisfy for $n \geq 0$ the three-term recurrence relation (e.g. Erdélyi *et al.* 1953, p. 158; Szegö 1975, p. 42)

$$p_{n+1}(\lambda) = (A_n \lambda + B_n) p_n(\lambda) - C_n p_{n-1}(\lambda) \tag{2.7}$$

with $C_0 = 0$ and

$$A_n := \frac{k_{n+1}}{k_n}, B_n := A_n \left(\frac{k'_{n+1}}{k_{n+1}} - \frac{k'_n}{k_n} \right), C_n := \frac{A_n h_n}{A_{n-1} h_{n-1}}, \tag{2.8}$$

where

$$p_n(\lambda) = k_n \lambda^n + k'_n \lambda^{n-1} + \ldots \text{and } h_n := (p_n, p_n). \tag{2.9}$$

The mathematical basis for the representation of $c(\zeta)$ by a stack of thin sheets is Markoff's theorem (Markoff 1895), presented here in the formulation of Erdélyi et al. (1953, p. 162); see also Szegö (1975, p. 54) and Perron (1913, § 68). Markoff's theorem expresses $c(\zeta)$ as a CF in terms of A_n, B_n and C_n as

$$c(\zeta) = \int_0^\infty \frac{w(\lambda) d\lambda}{\lambda + \zeta} = \cfrac{s_0 A_0}{A_0 \zeta - B_0 - \cfrac{C_1}{A_1 \zeta - B_1 - \cfrac{C_2}{A_2 \zeta - B_2 - \ldots}}}. \tag{2.10}$$

This CF representation converges in the whole ζ-plane with the exception of the points $\zeta = -\lambda$ with $w(\lambda) > 0$.

In addition to the contracted CF (2.10), we consider also its even extension, defined by the property that the approximant of order m of the contracted CF agrees with the approximant of order $2m$ of the extended CF, $m = 1, 2, 3, \ldots$. Then contracted and extended CFs are given by (e.g. Wall 1948, p. 21)

$$c(\zeta) = \cfrac{a_0}{A_0\zeta + b_0 - \cfrac{b_0 a_1}{A_1\zeta + a_1 + b_1 - \cfrac{b_1 a_2}{A_2\zeta + a_2 + b_2 - \ldots}}} \tag{2.11}$$

$$= \cfrac{a_0/A_0}{\zeta + \cfrac{b_0/A_0}{1 + \cfrac{a_1/A_1}{\zeta + \cfrac{b_1/A_1}{1 + \cfrac{a_2/A_2}{\zeta + \ldots}}}}}, \tag{2.12}$$

where the comparison of eqs (2.10) and (2.11) yields

$$a_0 = s_0 A_0, b_0 = -B_0, b_{n-1}a_n = C_n, a_n + b_n = -B_n, n \geq 1. \tag{2.13}$$

Contraction and extension are illustrated by verifying that, for instance, the approximant $m = 2$ of eq. (2.11) agrees with the approximant $2m = 4$ of eq. (2.12):

$$\cfrac{a_0}{A_0\zeta + b_0 - \cfrac{b_0 a_1}{A_1\zeta + a_1 + b_1}} = \cfrac{a_0/A_0}{\zeta + \cfrac{b_0/A_0}{1 + \cfrac{a_1/A_1}{\zeta + b_1/A_1}}}. \tag{2.14}$$

Solving eq. (2.13) for a_n and b_n, we obtain for $n \geq 1$

$$a_n = -\cfrac{C_n}{B_{n-1} - \cfrac{C_{n-1}}{B_{n-2} - \ldots - \cfrac{C_1}{B_0}}}, b_n = -B_n - a_n, \tag{2.15}$$

and deduce from eq. (2.7)

$$a_n = -C_n p_{n-1}(0)/p_n(0), \quad n \geq 1, \tag{2.16}$$

and

$$b_n = -p_{n+1}(0)/p_n(0), \quad n \geq 0. \tag{2.17}$$

Moreover, $a_0 = s_0 A_0$. Recalling that $w(\lambda) \equiv 0$ for $\lambda < 0$, all n zeros of $p_n(\lambda)$ lie in $\lambda > 0$ (e.g. Szegö 1975, p. 44). Therefore, no sign changes of $p_n(\lambda)$ can occur in $\lambda \leq 0$ and $\text{sign}[p_n(\lambda)/k_n] = (-1)^n$ for $\lambda \to -\infty$ implies $\text{sign}[p_n(0)/k_n] = (-1)^n$. With eqs (2.8), (2.16) and (2.17) it then follows that $a_n/A_n > 0$ and $b_n/A_n > 0$. This positivity warrants the further substitutions

$$\frac{a_n}{A_n} = \frac{1}{\mu_0 \tau_n d_n}, \quad \frac{b_n}{A_n} = \frac{1}{\mu_0 \tau_n d_{n+1}}, \quad n \geq 0, \tag{2.18}$$

with the understanding that $a_0/A_0 = 1/(\mu_0 \tau_0)$. The inversion of eq. (2.18) yields

$$\mu_0 \tau_n = \frac{b_0 b_1 \ldots b_{n-1}}{a_0 a_1 \ldots a_n} \cdot A_n > 0, \quad d_{n+1} = \frac{a_0 a_1 \ldots a_n}{b_0 b_1 \ldots b_n} > 0, \quad n \geq 0. \tag{2.19}$$

The new parameters τ_n and d_n will turn out to be the intrinsically positive thin-sheet parameters. The substitutions (2.18) transform the CF (2.12) into (*cf.* Perron 1913, § 67)

$$c(\zeta) = \cfrac{1}{\mu_0\tau_0\zeta + \cfrac{1}{d_1 + \cfrac{1}{\mu_0\tau_1\zeta + \cfrac{1}{d_2 + \ldots}}}}. \tag{2.20}$$

This CF represents the response of a stack of thin sheets (*cf.* Fig. 2) because the response functions c_n and c_{n+1} at levels z_n^- and z_{n+1}^- (i.e. immediately above the sheets) are recursively connected by

$$\frac{1}{c_n} = \mu_0 \tau_n \zeta + \frac{1}{d_{n+1} + c_{n+1}}. \tag{2.21}$$

Concatenating these recursion formulae, starting with $c(\zeta) =: c_0$, we arrive at the CF (2.20). Finally, the result quoted in eqs (2.5) and (2.6) is obtained by inserting eqs (2.16) and (2.17) into eq. (2.19) on using eq. (2.8) and $h_0 = p_0^2 s_0 = p_0^2 a_0/A_0$.

If $w(\lambda)$ has an infinite number of points, where $w(\lambda) > 0$, the CF (2.20) is infinite. This occurs, for instance, if there exists at least one section where $0 \leq a < \lambda < b$, $w(\lambda) > 0$ or if $w(\lambda)$ is a superposition of an infinite number of δ-functions at the discrete points λ_m.

The CF is finite, if $w(\lambda)$ consists of a finite number N of δ-functions. The termination of the CF (2.20) will be demonstrated for the example (1.9), assuming more generally $\lambda \geq 0$. The scalar product (2.2) now reads explicitly

$$(f, g) := \sum_{m=1}^{N} w_m f(\lambda_m) g(\lambda_m). \tag{2.22}$$

Therefore $p_N(\lambda)$, being orthogonal to the N polynomials up to degree $N-1$, is simply

$$p_N(\lambda) = k_N \prod_{\ell=1}^{N} (\lambda - \lambda_\ell), \tag{2.23}$$

implying $h_N = (p_N, p_N) = 0$. If $\min(\lambda_m) > 0$, then $p_N(0) \neq 0$ and $\tau_N = \infty$. If, however, $\min(\lambda_m) = 0$, then $p_N(0) = 0$ and $d_N = \infty$ (i.e. the conductor terminates with the finite conductance τ_{N-1}). In this case, regular orthogonal polynomials exist only up to degree $N-1$, whereas no normalization is possible for degree $n \geq N$.

2.2 A numerical algorithm

For numerical simplicity, the orthogonal polynomials $p_n(\lambda)$ with the weight function $w(\lambda)$ are now assumed to be normalized, i.e.

$$h_n = (p_n, p_n) = 1, k_n > 0. \tag{2.24}$$

Then the three-term recurrence relation (2.7) reads on using eq. (2.8)

$$\beta_{n+1} p_{n+1}(\lambda) = (\lambda - \alpha_n) p_n(\lambda) - \beta_n p_{n-1}(\lambda), \tag{2.25}$$

where $\beta_{n+1} := 1/A_n = k_n/k_{n+1} > 0$ and $\alpha_n := (\lambda\ p_n, p_n)$. The value of α_n follows from eqs (2.24) and (2.25) observing that $p_{n-1}(\lambda)$ and $p_{n+1}(\lambda)$ are orthogonal to $p_n(\lambda)$. Eq. (2.25) opens a simple way for the recursive computation of the polynomials: starting with

$$p_{-1}(\lambda) := 0,\ p_0(\lambda) := 1/\sqrt{s_0},\ \beta_0 := 0, \tag{2.26}$$

we obtain for $n = 0, 1, 2, \ldots$

(i) $\alpha_n := (\lambda p_n, p_n)$,
(ii) $\tilde{p}_{n+1}(\lambda) := (\lambda - \alpha_n) p_n(\lambda) - \beta_n p_{n-1}(\lambda)$,
(iii) $\beta_{n+1} := \sqrt{(\tilde{p}_{n+1}, \tilde{p}_{n+1})}$,
(iv) $p_{n+1}(\lambda) := \tilde{p}_{n+1}(\lambda)/\beta_{n+1}$

Taking into account that $h_n = 1$, $k_n/k_{n+1} = \beta_{n+1}$, eqs (2.5) and (2.6) simplify to

$$\mu_0 \tau_n = p_n^2(0), n \geq 0, \tag{2.27}$$

$$d_{n+1} = -\frac{1}{p_n(0)\tilde{p}_{n+1}(0)}, n \geq 0. \tag{2.28}$$

In step (ii) and (iv) of the algorithm, $\tilde{p}_{n+1}(0)$ and $p_{n+1}(0)$ are updated along with $\tilde{p}_{n+1}(\lambda)$ and $p_{n+1}(\lambda)$. The spectral function $w(\lambda)$ enters in step (i) and step (iii).

Again the finite discrete case (1.9) deserves special attention. Because $\beta_N\ k_N = k_{N-1}$, equation (2.23) implies

$$\tilde{p}_N(\lambda) = k_{N-1} \prod_{\ell=1}^{N} (\lambda - \lambda_\ell). \tag{2.29}$$

First let $\min(\lambda_m) = 0$. Then $\tilde{p}_N(0) = 0$ and therefore $d_N = \infty$, meaning that the conductor terminates with τ_{N-1}. Now let $\min(\lambda_m) > 0$. In view of the normalization $h_N = 1$, the polynomial $p_N(\lambda)$ given in eq. (2.23) demands that $k_N = \infty$, resulting in $p_N(0) = \infty$ and $\tau_N = \infty$.

For the finite discrete case, the performance of the present algorithm was compared with the performance of the Rutishauser algorithm proposed by Parker & Whaler (1981). This algorithm transforms the frequency domain partial fraction (1.12) into a CF of type (2.20). Even for complicated models with 50 to 70 sheets, no difference was detected. This means that the algorithm described is both simple and stable.

2.3 Expression of the sheet parameters in terms of the moments

In the previous two sections, the sheet parameters were expressed in terms of orthogonal polynomials $p_n(\lambda)$ generated by $w(\lambda)$. As an alternative, the sheet parameters can be expressed in terms of the moments s_k of $w(\lambda)$. This presentation requires the determinants $\Delta_n(i)$, $i = 0, 1$, defined by $\Delta_0(i) := 1$ and

$$\Delta_n(i) := \begin{vmatrix} s_i & s_{i+1} & \ldots & s_{i+n-1} \\ s_{i+1} & s_{i+2} & \ldots & s_{i+n} \\ \ldots & \ldots & \ldots & \ldots \\ s_{i+n-1} & s_{i+n} & \ldots & s_{i+2n-2} \end{vmatrix}, \quad n \geq 1. \tag{2.30}$$

Here, $\Delta_n(i)$ is an nth order determinant with the element s_i in the upper left corner. A determinant, in which the entry (j, k) depends on $j + k$ only, is called a Hankel determinant. If there is an infinite number of points with $w(\lambda) > 0$, then $\Delta_n(i) > 0$ for all n. This is immediately obvious from the fact that the positive-definite quadratic form

$$\int_{0^-}^{\infty} w(\lambda)\lambda^i \left(\sum_{j=0}^{n-1} \lambda^j u_j\right)^2 d\lambda = \sum_{j,k=0}^{n-1} s_{i+j+k} u_j u_k \tag{2.31}$$

requires $\det[s_{i+j+k}]_{j,k=0,\ldots,n-1} = \Delta_n(i) > 0$. The finite discrete case (1.9) will be considered at the end of this section.

Then the presentation of the sheet parameters in terms of the moments is

$$\mu_0\tau_n = \frac{\Delta_n^2(1)}{\Delta_n(0)\Delta_{n+1}(0)}, n \geq 0, \tag{2.32}$$

$$d_{n+1} = \frac{\Delta_{n+1}^2(0)}{\Delta_n(1)\Delta_{n+1}(1)}, n \geq 0. \tag{2.33}$$

These results are also quoted by Shohat & Tamarkin (1943, p. 73), referring to Perron (1913). The first few sheet parameters are

$$\mu_0\tau_0 = \frac{1}{s_0}, \quad d_1 = \frac{s_0^2}{s_1}, \quad \mu_0\tau_1 = \frac{s_1^2}{s_0\left(s_0 s_2 - s_1^2\right)}, \quad d_2 = \frac{\left(s_0 s_2 - s_1^2\right)^2}{s_1\left(s_1 s_3 - s_2^2\right)}. \tag{2.34}$$

This example clearly shows how the number of required moments increases with increasing depth of investigation: all moments up to order $2n$ and $2n + 1$, respectively, are required to recover τ_n and d_{n+1}, $n = 0, 1, 2, \ldots$.

We shall derive eqs (2.32) and (2.33) from eqs (2.5) and (2.6) on using for $p_n(\lambda)$ its representation in terms of the moments: let

$$p_n(\lambda) = \sum_{j=0}^{n} a_{nj}\lambda^j, \tag{2.35}$$

where $a_{nn} =: k_n \neq 0$ is taken as a free scaling factor at our disposal. In particular, $p_0(\lambda) = k_0$. For $n \geq 1$, the remaining n coefficients a_{nj} are determined from the n conditions

$$(\lambda^m, p_n) = 0, \quad m = 0, \ldots, n-1 \tag{2.36}$$

implied in the n orthogonality conditions $(p_\ell, p_n) = 0$, $\ell = 0, \ldots, n-1$. From eqs (2.35) and (2.36) result the n equations

$$\sum_{j=0}^{n-1} a_{nj} s_{j+m} = -k_n s_{n+m}, m = 0, \ldots, n-1. \tag{2.37}$$

Solving for a_{nj} and inserting in eq. (2.35), we obtain for $n \geq 1$

$$p_n(\lambda) = \frac{k_n}{\Delta_n(0)} \begin{vmatrix} s_0 & s_1 & \ldots & s_{n-1} & s_n \\ s_1 & s_2 & \ldots & s_n & s_{n+1} \\ \ldots & \ldots & \ldots & \ldots & \ldots \\ s_{n-1} & s_n & \ldots & s_{2n-2} & s_{2n-1} \\ 1 & \lambda & \ldots & \lambda^{n-1} & \lambda^n \end{vmatrix} \tag{2.38}$$

(Erdélyi et al. 1953, p. 158). Obviously, the co-factor of λ^n is k_n and eq. (2.36) is satisfied because, after insertion of p_n and integration, the $(n + 1)$th row of the resulting determinant duplicates one of the n upper rows and therefore the determinant vanishes.

Following Wimp (2000, p. 191), we deduce from eq. (2.38) for $\lambda = 0$

$$p_n(0) = (-1)^n k_n \Delta_n(1)/\Delta_n(0). \tag{2.39}$$

Moreover, using eq. (2.38),

$$h_n = (p_n, p_n) = k_n(\lambda^n, p_n) = k_n^2 \Delta_{n+1}(0)/\Delta_n(0). \tag{2.40}$$

After eliminating with eqs (2.39) and (2.40) the quantities $p_n(0)$, k_n and h_n from eqs (2.5) and (2.6), we arrive at eqs (2.32) and (2.33). A derivation of these equations without appeal to orthogonal polynomials is given in Appendix A.

The expression of the cumulative parameters

$$S_n := \sum_{\ell=0}^{n} \tau_\ell, n \geq 0, \quad z_0 := 0, \quad z_n := \sum_{\ell=1}^{n} d_\ell, \quad n \geq 1, \tag{2.41}$$

in terms of the moments is particularly simple,

$$\mu_0 S_n = \frac{\Delta_n(2)}{\Delta_{n+1}(0)}, \quad z_n = -\frac{\Delta_{n+1}(-1)}{\Delta_n(1)}, \quad n \geq 0. \tag{2.42}$$

The determinants $\Delta_n(2)$ and $\Delta_n(-1)$ are also defined by eq. (2.30) with $i = 2$ and $i = -1$. In the latter case, the additional definition $s_{-1} := 0$ applies. The relations (2.42) are proved by first verifying that $S_0 = \tau_0$ and $z_0 = 0$, and then considering $S_n - S_{n-1} = \tau_n$ and $z_n - z_{n-1} = d_n$, $n \geq 1$, on using the identity (Pólya & Szegö 1971, problem VII,19)

$$\Delta_k(i-1)\Delta_k(i+1) - \Delta_{k+1}(i-1)\Delta_{k-1}(i+1) = \Delta_k^2(i). \tag{2.43}$$

For the finite discrete case (1.9), for which eqs (2.32) and (2.33) deserve special attention, the pertinent results are summarized only: the determinants $\Delta_n(i)$ are positive for $n \leq N-1$ and vanish for $n \geq N+1$. For $n = N$, we have $\Delta_N(0) > 0$ and either $\Delta_N(1) > 0$ if $\min(\lambda_m) > 0$ or $\Delta_N(1) = 0$ if $\min(\lambda_m) = 0$. From eqs (2.32) and (2.33), it then follows that the stack of thin sheets ends for $\min(\lambda_m) > 0$ with $\tau_N = \infty$ and for $\min(\lambda_m) = 0$ with $d_N = \infty$ (i.e. with the finite conductance τ_{N-1}).

The expressions of the sheet parameters by the moments via eqs (2.32) and (2.33) are of formal simplicity. This holds in particular also for the cumulative parameters (2.42). However, compared with the orthogonal polynomial approach, they are less suitable for a quantitative determination of the parameters from a given spectral function, because the evaluation of determinants is awkward and not very stable without precautions.

2.4 The sequence of thin sheets generated by the classical orthogonal polynomials

In this section, we shall study the thin-sheet structures associated with the classical continuous and discrete orthogonal polynomials. A wealth of information about these polynomials is contained in Erdélyi et al. (1953, chapter 10), Abramowitz & Stegun (1972, chapter 22), Szegö (1975). The easily accessible middle reference will satisfy most needs.

The weight function (spectral function) $w(\lambda)$ is parametrized by its zero-order moment $s_0 > 0$ as a free parameter at our disposal. From eq. (2.34) follows $s_0 = 1/(\mu_0 \tau_0)$ with τ_0 as conductance of the surface sheet.

2.4.1 Continuous weight function $w(\lambda)$

Here, only Legendre and Chebyshev polynomials are considered, which are members of the wide class of Jacobi polynomials treated in some detail in Appendix C.

Legendre polynomials. The weight and response functions of the Legendre polynomials $P_n(x)$, $-1 \leq x \leq +1$, shifted to the interval $0 \leq a \leq \lambda \leq b$, $b > a$, are

$$w(\lambda) = \frac{s_0}{b-a}, \quad c(\zeta) = \frac{s_0}{b-a} \log\left(\frac{b+\zeta}{a+\zeta}\right), \tag{2.44}$$

where eq. (1.4) has been used. The associated polynomials

$$p_n(\lambda) = P_n\left(\frac{2\lambda - a - b}{b-a}\right) \tag{2.45}$$

satisfy

$$p_n(0) = P_n(-u) = (-1)^n P_n(u), \quad u := (b+a)/(b-a) \geq 1 \tag{2.46}$$

and

$$h_n = \frac{s_0}{2n+1}, \quad \frac{k_{n+1}}{k_n} = \frac{2}{b-a} \cdot \frac{2n+1}{n+1}. \tag{2.47}$$

Therefore, eqs (2.5) and (2.6) yield the sheet parameters

$$\mu_0 \tau_n = (2n+1)[P_n(u)]^2/s_0, \, n \geq 0, \tag{2.48}$$

$$d_{n+1} = 2s_0/[(b-a)(n+1)P_n(u)P_{n+1}(u)], \, n \geq 0. \tag{2.49}$$

This is an infinite sequence of thin sheets with increasing conductance τ_n and decreasing separation d_n, clustering at $z_\infty = c(0) = s_0(b-a)^{-1} \log(b/a)$. For $a = 0$, implying $u = 1$, $P_n(1) = 1$, the structure simplifies to $\mu_0 \tau_n = (2n+1)/s_0$, $d_{n+1} = 2s_0/[(n+1)\, b]$, $n \geq 0$.

Chebyshev polynomials. The weight function of the Chebyshev polynomials of the first kind, $T_n(x) = \cos(n \arccos x)$, shifted from the interval $-1 < x < +1$ to the interval $0 \leq a < \lambda < b$, is

$$w(\lambda) = \frac{s_0}{\pi\sqrt{(\lambda - a)(b - \lambda)}}, \quad a < \lambda < b. \tag{2.50}$$

Outside this interval, $w(\lambda) = 0$. According to eq. (1.4), $w(\lambda)$ gives rise to the response function

$$c(\zeta) = \frac{s_0}{\sqrt{(a+\zeta)(b+\zeta)}}. \tag{2.51}$$

The associated polynomials are

$$p_n(\lambda) = T_n\left(\frac{2\lambda - a - b}{b-a}\right) \tag{2.52}$$

with

$$p_n(0) = T_n(-u) = (-1)^n T_n(u), \quad u := (b+a)/(b-a) \geq 1 \tag{2.53}$$

and

$$h_n = \begin{cases} s_0, & n = 0 \\ s_0/2, & n \geq 1 \end{cases}, \quad \frac{k_{n+1}}{k_n} = \frac{2}{b-a} \cdot \begin{cases} 1, & n = 0 \\ 2, & n \geq 1 \end{cases}. \tag{2.54}$$

Therefore, eqs (2.5) and (2.6) give the sheet parameters

$$\mu_0 \tau_n = 1/s_0, n = 0 \quad \text{and} \quad \mu_0 \tau_n = 2[T_n(u)]^2/s_0, n \geq 1, \tag{2.55}$$

$$d_{n+1} = 2s_0/[(b-a)T_n(u)T_{n+1}(u)], n \geq 0. \tag{2.56}$$

For $a > 0$, this is again an infinite sequence of thin sheets with increasing conductance τ_n and decreasing separation d_n, clustering at $z_\infty = c(0) = s_0/\sqrt{ab}$. For $a = 0$, implying $u = 1$, $T_n(1) = 1$, we obtain the simple structure $\mu_0 \tau_n = 1/s_0$ for $n = 0$, $\mu_0 \tau_n = 2/s_0$ for $n \geq 1$ and $d_{n+1} = 2s_0/b$ for $n \geq 0$.

The last conductivity model has an interesting application: if displacement currents are taken into account, the response function of a uniform half-space with conductivity σ and permittivity ϵ is

$$c(\zeta) = \frac{1}{\sqrt{\zeta \mu_0 (\sigma + \zeta \epsilon)}}, \tag{2.57}$$

which has the form of eq. (2.51) with $a = 0$, $b = \sigma/\epsilon$ and $s_0 = 1/\sqrt{\epsilon \mu_0}$. If erroneously a quasi-static interpretation of $c(\zeta)$ is attempted, one would get instead of a uniform dispersive half-space an almost uniformly laminated conductor with $\tau_0 = \sqrt{\epsilon/\mu_0}$, $\tau_n = 2\tau_0$, $n \geq 1$ and $d_{n+1} = D$, $n \geq 0$, where $D := (2/\sigma)\sqrt{\epsilon/\mu_0}$. The average conductivity, $2\tau_0/D$, agrees with the true conductivity. The length D is the high-frequency limit of the penetration depth,

$$1/D = \lim_{\omega \to \infty} \Re \sqrt{i\omega\mu_0(\sigma + i\omega\epsilon)} \tag{2.58}$$

(where $\Re$ denotes the real part), and $1/\tau_0$ is the plane-wave impedance ($= 377\ \Omega$ for $\epsilon = \epsilon_0$). Numerical values for $\epsilon = 9\epsilon_0$, $\sigma = 0.01$ S m^{-1} are $\tau_0 = 0.008$ S, $D = 1.6$ m.

An asymptotic result. In this section, it is shown that for $n \gg 1$ the sheet parameters follow a very simple pattern, only weakly influenced by the actual choice of the weight function. For $w(\lambda) > 0$ in $0 < a < \lambda < b$ and $v := (\sqrt{b} + \sqrt{a})/(\sqrt{b} - \sqrt{a}) > 1$, we have

$$\mu_0 \tau_n = v^{2n} F(v, w)/s_0, n \gg 1, \tag{2.59}$$

$$d_{n+1} = \frac{4s_0}{(b-a)v^{2n+1}F(v, w)}, n \gg 1, \tag{2.60}$$

where the non-dimensional function $F > 0$ is independent of n.

For a proof of eqs (2.59) and (2.60), let $R_n(x)$ be an orthogonal polynomial associated with the positive weight function $\tilde{w}(x)$, where $-1 < x < +1$. For formal simplicity, the standardization

$$\int_{-1}^{+1} \tilde{w}(x)\, dx = 1 \tag{2.61}$$

is applied. The polynomial $R_n(x)$ is assumed to be normalized, i.e. $\tilde{h}_n = 1$ and $\tilde{k}_n > 0$. Let x be real with $|x| > 1$ and let y be the solution of $y^2 - 2xy + 1 = 0$ with $|y| > 1$, i.e. $y = x + \sqrt{x^2 - 1}$ for $x > 1$ and $y = -(|x| + \sqrt{x^2 - 1})$ for $x < -1$. Then for $n \gg 1$ we have asymptotically, adapted from Szegö (1975, p. 277 and 297),

$$R_n(x) \simeq y^n \cdot G(y) \tag{2.62}$$

with

$$G(y) = \frac{1}{\sqrt{2\pi}} \exp\left\{ -\frac{y^2 - 1}{2\pi} \int_{-1}^{+1} \frac{\log[\tilde{w}(t)\sqrt{1 - t^2}]}{y^2 - 2yt + 1} \cdot \frac{dt}{\sqrt{1 - t^2}} \right\}, \tag{2.63}$$

or alternatively (Gradshteyn & Ryzhik 1980, integral 4.384.15)

$$G(y) = \frac{|y|}{\sqrt{\pi(y^2 - 1)}} \exp\left[-\frac{y^2 - 1}{2\pi} \int_{-1}^{+1} \frac{\log \tilde{w}(t)}{y^2 - 2yt + 1} \cdot \frac{dt}{\sqrt{1 - t^2}} \right]. \tag{2.64}$$

In particular,

$$G(y) = \frac{|y|}{\sqrt{(\pi/2)(y^2 - 1)}} \quad \text{for} \quad \tilde{w}(t) = \frac{1}{2} \quad \text{(Legendre)} \tag{2.65}$$

and

$$G(y) = \frac{1}{\sqrt{2}} \quad \text{for} \quad \tilde{w}(t) = \frac{1}{\pi\sqrt{1 - t^2}} \quad \text{(Chebyshev)}. \tag{2.66}$$

Generally, $G(y)$ is symmetric around $y = 0$ if $\tilde{w}(t)$ is symmetric around $t = 0$.

Our application requires the shifted polynomial

$$p_n(\lambda) = R_n\left(\frac{2\lambda - a - b}{b - a}\right), 0 < a < \lambda < b, \tag{2.67}$$

with the weight function, taking into account eq. (2.61),

$$w(\lambda) = \frac{2s_0}{b - a} \cdot \tilde{w}\left(\frac{2\lambda - a - b}{b - a}\right). \tag{2.68}$$

Of interest is $p_n(0) = R_n(x)$ with

$$x = -u, u = \frac{b + a}{b - a} > 1 \quad \text{and} \quad y = -v, v = \frac{\sqrt{b} + \sqrt{a}}{\sqrt{b} - \sqrt{a}} > 1. \tag{2.69}$$

From eq. (2.64) it is inferred that the coefficient $\tilde{k}_n$ of the highest power x^n of $R_n(x)$ is for $n \gg 1$ (Szegö 1975, p. 309)

$$\tilde{k}_n = \lim_{x\to\infty} \frac{R_n(x)}{x^n} = \frac{2^n}{\sqrt{\pi}} \exp\left[-\frac{1}{2\pi}\int_{-1}^{+1} \frac{\log \tilde{w}(t)\, dt}{\sqrt{1 - t^2}}\right], \tag{2.70}$$

observing that $y \to 2x$. Therefore, $\tilde{k}_{n+1}/\tilde{k}_n \simeq 2$ and

$$\frac{k_{n+1}}{k_n} = \frac{2}{b - a} \cdot \frac{\tilde{k}_{n+1}}{\tilde{k}_n} \simeq \frac{4}{b - a}. \tag{2.71}$$

With $h_n = s_0$, we obtain from eqs (2.5) and (2.6)

$$\mu_0\tau_n = v^{2n}[G(-v)]^2/s_0, n \gg 1, \tag{2.72}$$

$$d_{n+1} = \frac{4s_0}{(b - a)v^{2n+1}[G(-v)]^2}, n \gg 1, \tag{2.73}$$

implying

$$T_n := \mu_0\tau_n d_{n+1} = \frac{4}{(b - a)v} = \frac{4}{(\sqrt{a} + \sqrt{b})^2}, n \gg 1, \tag{2.74}$$

which becomes independent of the weight function and of n, and is valid also in the limits $a \to 0$ and $a \to b$. The time T_n can be considered as a local decay time of the conducting sheet τ_n separated by d_{n+1} from a deeper perfect conductor. For $a/b > 0.1$ and $n > 10$, the approximations (2.72) and (2.73) are correct to within 5 per cent for Legendre polynomials and to within 0.001 per cent for Chebyshev polynomials.

The asymptotic treatment shows that the sheet parameters are controlled by the quantity v, whereas the actual behaviour of the weight function $w(\lambda)$, involved in $G(-v)$, plays a surprisingly insignificant role. For $a > 0$, the conductances monotonically increase in a geometric progression and the distances between sheets decrease with the reverse law. Therefore, the sheets converge to a perfect conductor at finite depth. In its character, this thin-sheet structure does not differ much from that of a single discrete line ($a \to b$), giving rise to a surface sheet and a perfect conductor at finite depth. The spectral function for the complementary sequence of thin sheets with decreasing conductances and increasing separations requires an additional spectral line at $\lambda = 0$. This model is discussed in Section 2.5.

Laguerre polynomials. Contrary to the previous examples, the polynomials are now defined in the full range $0 \le \lambda < \infty$. Weight function and response function are

$$w(\lambda) = s_0 a \mathrm{e}^{-a\lambda}, \quad c(\zeta) = s_0 a \mathrm{e}^{a\zeta}\mathrm{E}_1(a\zeta), \tag{2.75}$$

where $a > 0$ is a scaling factor and

$$\mathrm{E}_1(z) = \int_z^\infty \mathrm{e}^{-t}\frac{dt}{t}, |\arg z| < \pi \tag{2.76}$$

is the exponential integral with a branch cut along the negative-real semi-axis. The moments s_k, defined in eq. (1.13), are $s_k = s_0\, k!/a^k$. Therefore in this infinite range, the high frequency expansion (A9) is valid only asymptotically. The first few terms are

$$c(\zeta) = \frac{s_0}{\zeta}\left[1 - \frac{1!}{a\zeta} + \frac{2!}{(a\zeta)^2} - \cdots\right]. \tag{2.77}$$

The weight function $w(\lambda)$ generates the orthogonal Laguerre polynomials

$$p_n(\lambda) = L_n(a\lambda) \quad \text{with} \quad p_n(0) = 1. \tag{2.78}$$

Because

$$h_n = s_0, \quad k_{n+1}/k_n = -a/(n + 1), \tag{2.79}$$

the sheet parameters (2.5), (2.6) are simply

$$\mu_0\tau_n = 1/s_0, \quad d_{n+1} = s_0 a/(n + 1), n \ge 0. \tag{2.80}$$

2.4.2 Completely discrete weight function $w(\lambda)$

These polynomials $p_n(\lambda)$ are orthogonal with respect to a finite or infinite set of discrete abscissae λ_m and weights w_m, i.e. the weight function and orthogonality relation are

$$w(\lambda) = \sum_m w_m \delta(\lambda - \lambda_m), \quad \sum_m w_m p_n(\lambda_m) p_j(\lambda_m) = h_n \delta_{nj}. \tag{2.81}$$

The response function is simply

$$c(\zeta) = \sum_m \frac{w_m}{\lambda_m + \zeta}. \tag{2.82}$$

Discrete Legendre polynomials. The polynomials $p_n(\lambda)$ are shifted versions of the discrete Legendre polynomials $\Pi_n(x|N) =: \Pi_n(x)$, $0 \le n \le N-1$, briefly described in Appendix D. They are orthogonal on a finite set of N equidistant abscissae

$$\lambda_m = a + m(b-a)/(N-1), 0 \le m \le N-1, \tag{2.83}$$

with equal weights $w_m = s_0/N$ and are given by

$$p_n(\lambda) = \Pi_n\left(\frac{2\lambda - a - b}{b-a}\right), 0 \le a \le \lambda \le b, \quad b > a, \tag{2.84}$$

with

$$p_n(0) = \Pi_n(-u) = (-1)^n \Pi(u), u := (b+a)/(b-a) \ge 1. \tag{2.85}$$

The polynomial parameters are

$$h_n = \frac{s_0}{2n+1} \cdot \prod_{m=0}^{n} \frac{N+m}{N-m}, \quad \frac{k_{n+1}}{k_n} = \frac{2}{b-a} \cdot \frac{(2n+1)(N-1)}{(n+1)(N-n-1)}, \tag{2.86}$$

converging for $N \to \infty$ to eq. (2.47). From eqs (2.5) and (2.6) follow the sheet parameters

$$\mu_0 \tau_n = [\Pi_n(u)]^2 / h_n, 0 \le n \le N-1, \tag{2.87}$$

$$d_{n+1} = \frac{k_{n+1} h_n}{k_n \Pi_n(u) \Pi_{n+1}(u)}, 0 \le n \le N-2. \tag{2.88}$$

Moreover (see Appendix D),

$$d_N = \frac{2h_{N-1}}{(b-a)\Pi_{N-1}(u)[u\Pi_{N-1}(u) - \Pi_{N-2}(u)]}, \tau_N = \infty. \tag{2.89}$$

For $a = 0$, i.e. $u = 1$, we obtain $d_N = \infty$ and τ_N is missing.

Charlier polynomials. They are an example of an infinite set of discrete abscissae,

$$\lambda_m = m\Delta, \quad w_m = s_0 e^{-a} a^m / m!, \quad m = 0, 1, 2, \ldots, \tag{2.90}$$

where $\Delta > 0$ is the λ discretization and $a > 0$ is a non-dimensional scaling parameter. The associated Charlier polynomials are given by (e.g. Erdélyi et al. 1953, p. 226)

$$p_n(\lambda) = \sum_{r=0}^{n} (-1)^r \binom{n}{r} \binom{\lambda/\Delta}{r} \frac{r!}{a^r} \tag{2.91}$$

with $p_n(0) = 1$. The polynomial parameters

$$h_n = s_0 n!/a^n, k_{n+1}/k_n = -1/(a\Delta) \tag{2.92}$$

give rise to the sheet parameters

$$\mu_0 \tau_n = \frac{a^n}{n! s_0}, d_{n+1} = \frac{n! s_0}{a^{n+1}\Delta}, n \ge 0. \tag{2.93}$$

For $a < 1$ the conductances monotonically decrease, for $a > 1$ they first increase until $n \simeq a$ and then decrease. The sheet separations behave oppositely. With $b := \zeta/\Delta$ and Kummer's transformation (Abramowitz & Stegun 1972, formula 13.1.27), the response function (2.82) is

$$c(\zeta) = s_0 e^{-a} \sum_{m=0}^{\infty} \frac{a^m}{m!(\lambda_m + \zeta)} = \frac{s_0}{\zeta} \cdot e^{-a} M(b, b+1, a) = \frac{s_0}{\zeta} \cdot M(1, b+1, -a) = \frac{s_0}{\zeta} \cdot \sum_{m=0}^{\infty} \frac{(-a)^m}{(b+1)_m}, \tag{2.94}$$

where M is the Kummer function (Abramowitz & Stegun 1972, chapter 13) and $(x)_m$ is the Pochhammer symbol defined in eq. (C4). Hence, asymptotically for $|b| \gg 1$,

$$c(\zeta) = \frac{s_0}{\zeta}\left[1 - \frac{a}{b} + \frac{a(a+1)}{b^2} - \frac{a(a^2+3a+1)}{b^3} + \cdots\right]. \tag{2.95}$$

See the end of Appendix B for sufficient conditions under which an infinite discrete spectrum evolves.

2.5 Two examples of a more complex spectral function

In the previous examples with a continuous spectral function, this function was non-vanishing in only one interval. Now we present two simple examples of a spectral function $w(\lambda)$ with a slightly more complicated structure.

Continuous spectrum plus single spectral line. The addition of a single spectral line at $\lambda = 0$ can drastically change the thin-sheet pattern. This is discussed by considering instead of $w(\lambda)$ the weighted mean

$$w_\epsilon(\lambda) := \epsilon s_0 \delta(\lambda) + (1-\epsilon) w(\lambda), \quad 0 \le \epsilon \le 1, \tag{2.96}$$

with the response function

$$c_\epsilon(\zeta) = \epsilon s_0/\zeta + (1-\epsilon) c(\zeta), \tag{2.97}$$

where s_0 is the zero-order moment both of $w(\lambda)$ and of $w_\epsilon(\lambda)$.

The limit $\epsilon = 1$ describes simply a thin surface sheet with $\tau_0 = 1/(\mu_0 s_0)$, which can be considered as the extremal expression of a sequence with decreasing conductances and increasing separations. On the other hand, the limit $\epsilon = 0$ recovers the sheet parameters of $w(\lambda)$. Therefore, in the model class of sequences of thin sheets with increasing conductances and decreasing sheet separations, which were typical for the first two examples treated in Section 2.4, intermediate values of ϵ will generate the complementary sequence of sheet parameters with decreasing conductances and increasing separations.

The resulting modifications of the sheet parameters are simple: let

$$\Sigma_0(\epsilon) := 1, \quad \Sigma_n(\epsilon) := 1 + \epsilon \sum_{m=1}^{n} (\tau_m/\tau_0), \quad n \ge 1. \tag{2.98}$$

Then

$$\frac{\tau_0(\epsilon)}{\tau_0} = 1, \quad \frac{\tau_n(\epsilon)}{\tau_n} = \frac{1-\epsilon}{\Sigma_{n-1}(\epsilon)\Sigma_n(\epsilon)}, \quad \frac{d_n(\epsilon)}{d_n} = \frac{\Sigma_{n-1}^2(\epsilon)}{1-\epsilon}, \quad n \ge 1, \tag{2.99}$$

where τ_n and d_n refer to $w(\lambda)$ and $\tau_n(\epsilon)$ and $d_n(\epsilon)$ to $w_\epsilon(\lambda)$. With increasing ϵ, obviously $\tau_n(\epsilon)/\tau_n$ decreases, $d_n(\epsilon)/d_n$ increases, and for $\epsilon = 1$ only the surface sheet subsists.

This transformation is proved via the moment presentation of eqs (2.32) and (2.33) of the sheet parameters. Eq. (2.96) implies

$$s_0(\epsilon) = s_0, \, s_k(\epsilon) = (1-\epsilon) s_k, \, k \ge 1. \tag{2.100}$$

Therefore, the Hankel determinants (2.30) are modified as follows:

$$\Delta_n(i,\epsilon)/\Delta_n(i) = (1-\epsilon)^n, \, i \ge 1, \tag{2.101}$$

$$\Delta_n(0,\epsilon)/\Delta_n(0) = (1-\epsilon)^n \left[1 + \frac{\epsilon s_0}{1-\epsilon} \cdot \frac{\Delta_{n-1}(2)}{\Delta_n(0)}\right] = (1-\epsilon)^{n-1} \Sigma_{n-1}(\epsilon). \tag{2.102}$$

In the last step, we have made use of eq. (2.42). Then eqs (2.101) and (2.102) in conjunction with eqs (2.32) and (2.33) lead to eq. (2.99). Moreover, eq. (2.42) yields $S_n(\epsilon)/S_n = 1/\Sigma_n(\epsilon)$, whereas for $z_n(\epsilon)/z_n$ no simple expression exists. Invariant under a change of ϵ are the quantities

$$\tau_n^2(\epsilon) d_n(\epsilon) d_{n+1}(\epsilon) \quad \text{and} \quad \frac{1}{d_n(\epsilon)} \left[\frac{1}{\tau_{n-1}(\epsilon)} + \frac{1}{\tau_n(\epsilon)}\right], \, n \ge 1. \tag{2.103}$$

Bipartite continuous spectrum (*plus single spectral line*). This spectrum is related to the periodic structure $\tau_{2n} = \tau_a$ at $z_{2n} = 2nD$ and $\tau_{2n+1} = \tau_b$ at $z_{2n+1} = (2n+1)D$, $n \ge 0$. As inferred from eq. (2.20), the response function $c(\zeta)$ is implicitly defined by

$$c(\zeta) = \cfrac{1}{\mu_0 \tau_a \zeta + \cfrac{1}{D + \cfrac{1}{\mu_0 \tau_b \zeta + \cfrac{1}{D + c(\zeta)}}}} \tag{2.104}$$

and therefore reads explicitly

$$c(\zeta) = \frac{2 s_0 (\lambda_b + \zeta)}{\zeta(\lambda_b + \zeta) + \sqrt{\zeta(\lambda_a + \zeta)(\lambda_b + \zeta)(\lambda_c + \zeta)}} \tag{2.105}$$

with

$$s_0 := \frac{1}{\mu_0 \tau_a}, \, \lambda_a := \frac{2}{\mu_0 \tau_a D}, \, \lambda_b := \frac{2}{\mu_0 \tau_b D}, \, \lambda_c := \lambda_a + \lambda_b. \tag{2.106}$$

[The square root in eq. (2.105) has to be computed as the product of the square roots of the four factors of the radicand.] First let $\tau_a > \tau_b$, implying $\lambda_a < \lambda_b$. Then the spectral function, as deduced from eq. (1.11) with $\zeta = -\lambda + i0^+$, is

$$w(\lambda) = \frac{2s_0}{\pi\lambda_a} \cdot \begin{cases} \dfrac{\sqrt{(\lambda_a-\lambda)(\lambda_b-\lambda)(\lambda_c-\lambda)}}{(\lambda_c-2\lambda)\sqrt{\lambda}}, & 0 < \lambda \le \lambda_a, \\ \dfrac{\sqrt{(\lambda-\lambda_a)(\lambda-\lambda_b)(\lambda_c-\lambda)}}{(2\lambda-\lambda_c)\sqrt{\lambda}}, & \lambda_b \le \lambda \le \lambda_c. \end{cases} \tag{2.107}$$

The support of $w(\lambda)$ consists of two intervals of equal length λ_a, the zero $\lambda = \lambda_c/2$ of the denominator lies in the gap between these sections and therefore plays no significant role. The case $\tau_a < \tau_b$ or $\lambda_a > \lambda_b$ requires two modifications. First, the upper form of $w(\lambda)$ holds in the range $0 < \lambda \le \lambda_b$ and the lower form in the range $\lambda_a \le \lambda \le \lambda_c$. Secondly, $c(\zeta)$ now has a pole at $\zeta = -\lambda_c/2$, which augments the spectral function by

$$\Delta w(\lambda) = \frac{s_0(\lambda_a-\lambda_b)}{\lambda_a} \cdot \delta(\lambda - \lambda_c/2). \tag{2.108}$$

s_0 remains the zero-order moment of $w(\lambda)$. Taking into account that $2s_0/\lambda_a = D$, it is seen that the omission of the pole would result in the spectral function of a periodic structure starting with τ_b rather than $\tau_a(\tau_b > \tau_a)$. More obviously, this follows also from the identity

$$c(\zeta) = \frac{D\lambda_a(\lambda_b+\zeta)}{\zeta(\lambda_b+\zeta)+sqr} = \frac{D\lambda_b(\lambda_a+\zeta)}{\zeta(\lambda_a+\zeta)+sqr} + \frac{D(\lambda_a-\lambda_b)}{\lambda_c+2\zeta}, \tag{2.109}$$

where *sqr* denotes the square root in eq. (2.105).

In the particular case $\lambda_a = \lambda_b$, the two intervals coalesce and $w(\lambda)$ agrees with the Jacobian spectral function (C1) for $\alpha = -1/2$, $\beta = +1/2$, $a = 0$ and $b = \lambda_c$. In this limit, eq. (2.105) coincides with eq. (C15). The spectral function $w(\lambda)$ and the first polynomials are displayed in Fig. 3 for $\tau_a > \tau_b$ and in Fig. 4 for $\tau_a < \tau_b$. With $w(\lambda)$ given, the polynomials were obtained by the numerical method of Section 2.2. [Since τ_n and d_n are known in this example, analytical expressions are also easily obtained via eqs (B6) and (B10).]

If more generally the sheet parameters are p periodic, such that p is the smallest integer satisfying $\tau_{n+p} = \tau_n, d_{n+p} = d_n$ for all n, then for $p \ge 2$ the continuous spectrum consists of p disjoint sections with at most one spectral line in each of the gaps (Grommer 1914, pp. 151–152; Wouk 1953, pp. 156–157).

3 PIECEWISE CONTINUOUS CONDUCTIVITY STRUCTURES

3.1 The nature of the spectrum

Whereas in the previous section the conductor consisted of a finite or infinite stack of thin sheets, we are now considering the other extreme that no thin sheet is allowed to occur in the layering: the conductor consists of sections with continuous variation, possibly separated by interfaces where the conductivity changes discontinuously. For this class of conductivity models, the nature of the spectrum was studied by Weidelt (1972). The main results will now be summarized. Let z_m be the maximum depth to which an external electromagnetic field can

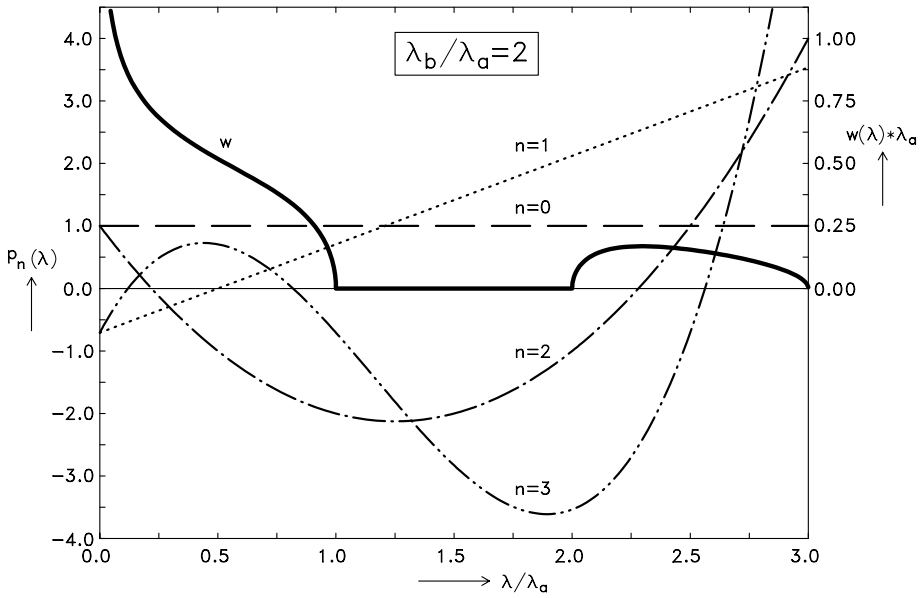

Figure 3. Weight function $w(\lambda)$ and the first orthogonal polynomials $p_n(\lambda)$ for a double-periodic sequence of sheets with the better conducting sheet at the surface ($\tau_a > \tau_b$ or $\lambda_a < \lambda_b$). The weight function is normalized with $s_0 = 1$.

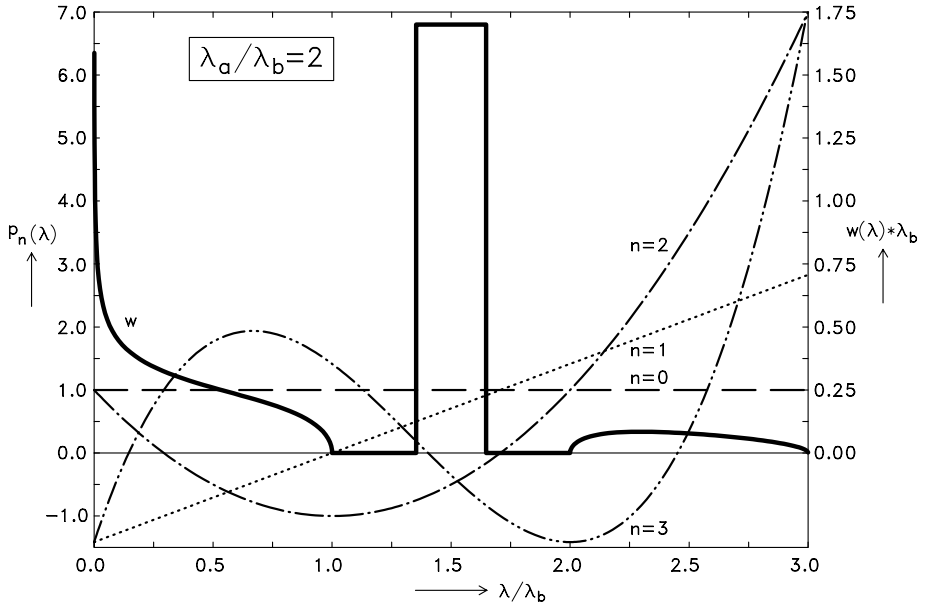

Figure 4. Weight function $w(\lambda)$ and the first orthogonal polynomials $p_n(\lambda)$ for a double-periodic sequence of sheets with the better conducting sheet at depth $z = D$ ($\tau_a < \tau_b$ or $\lambda_a > \lambda_b$). Now an additional spectral line occurs at $\lambda_c := (\lambda_a + \lambda_b)/2$. This line is displayed as a rectangular box with an arbitrary width, the area of the box, however, equals with the strength of the spectral line. Again the normalization $s_0 = 1$ is applied, to which in the present case the spectral line contributes 50 per cent and therefore exerts a great influence on the behaviour of $p_n(\lambda)$ near $\lambda = \lambda_c$ (compare with Fig. 3).

penetrate, i.e. z_m is either infinity, if the conductivity is bounded everywhere, or z_m is the finite depth below which infinite conductivity screens the electromagnetic field. The nature of the spectrum then depends on the integral

$$I := \int_0^{z_m} \sqrt{\sigma(z)}\, dz. \tag{3.1}$$

It is assumed that $0 < \sigma(0) < \infty$. The following two cases have to be considered.

(i) $I < \infty$: in this case, $c(\zeta)$ shows on the negative-real semi-axis an infinite number of poles at $\zeta = -\lambda_m$. For $m \gg 1$, poles and residuals are given by $\lambda_m \simeq m^2\pi^2/(\mu_0 I^2)$ and $w_m \simeq 2/[\mu_0\sqrt{\sigma(0)}I]$. Therefore

$$w(\lambda) = \sum_{m=1}^{\infty} w_m \delta(\lambda - \lambda_m) \quad \text{with} \quad \sum_{m=1}^{\infty} w_m = \infty. \tag{3.2}$$

The asymptotic behaviour of w_m follows from Weidelt (1972, p. 262) using the asymptotic theory of Morse & Feshbach (1953, p. 739).

(ii) $I = \infty$: the isolated poles beyond a certain limit point λ_B merge into a branch cut from $\zeta = -\lambda_B$ to $\zeta = -\infty$ with $w(\lambda) = \mathcal{O}(1/\sqrt{\lambda})$ for $\lambda \to \infty$. In $-\lambda_B \le \zeta \le 0$, a finite number of isolated poles or branch cuts of finite length may subsist.

In both cases no moment of $w(\lambda)$ exists. A few examples illustrate these results.

Uniform layer over perfect conductor or insulator. The layer of conductivity σ_0 and thickness D is the first lying over a perfect conductor. Then $I = \sqrt{\sigma_0}D$ is finite and

$$c(\zeta) = \frac{\tanh(\sqrt{\zeta\mu_0\sigma_0}D)}{\sqrt{\zeta\mu_0\sigma_0}} = \sum_{m=1}^{\infty} \frac{w_m}{\lambda_m + \zeta} \tag{3.3}$$

with

$$w_m = \frac{2}{\mu_0\sigma_0 D}, \lambda_m = \frac{(m - 1/2)^2\pi^2}{\mu_0\sigma_0 D^2}. \tag{3.4}$$

For $D \to \infty$, the poles coalesce and $c(\zeta)$ approaches the uniform half-space response $1/\sqrt{\zeta\mu_0\sigma_0}$ with a branch cut from $\zeta = 0$ to $\zeta = -\infty$. The changes for an underlying insulator are that tanh is replaced by coth, m-1/2 by m and a term $1/(\zeta\mu_0\sigma_0 D)$ is added in the series expansion.

Continuous conductivity variation $\sigma(z)$. In the model

$$\sigma = \sigma_0/\delta^4, \delta := 1 - bz, \tag{3.5}$$

quite different solutions are obtained for $b \ge 0$ and $b < 0$, corresponding to $I = \infty$ and $I < \infty$, respectively.

First, let $b \ge 0$. Then $\sigma \to \infty$ for $z \to 1/b$ and $I = \infty$. From eqs (1.2), (1.3) and (1.11), we find that the electric field, response function and spectral function are ($k^2 := \zeta\mu_0\sigma_0$)

$$E(z) \sim \delta \exp(-kz/\delta), c(\zeta) = \frac{1}{b + k}, w(\lambda) = \frac{1}{\pi} \cdot \frac{\sqrt{\lambda\mu_0\sigma_0}}{b^2 + \lambda\mu_0\sigma_0}. \tag{3.6}$$

Next let $b < 0$. Then $I = \sqrt{\sigma_0}/|b| < \infty$ and

$$E(z) \sim \delta \sinh\{k/(b\delta)\}, \quad c(\zeta) = \frac{1}{b - k\coth(k/b)} = \frac{3|b|}{\zeta\mu_0\sigma_0} + \sum_{m=1}^{\infty} \frac{w_m}{\lambda_m + \zeta}, \tag{3.7}$$

where

$$\lambda_m = \frac{(bx_m)^2}{\mu_0\sigma_0}, \; w_m = \frac{2|b|}{\mu_0\sigma_0}, \tag{3.8}$$

and x_m is the mth positive root of $x\cot x = 1$, implying $x_m \simeq (m + 1/2)\pi$ for $m \gg 1$.

Example of a branch cut with an isolated pole. Let $0 \le q \le p$ and consider the two responses

$$c_\pm(\zeta) = \frac{A}{\sqrt{\zeta + p} \pm \sqrt{q}}, \tag{3.9}$$

where A, of dimension m $s^{-1/2}$, is a positive constant. Both responses have a branch cut from $\zeta = -p$ to $\zeta = -\infty$. However, in addition, $c_-(\zeta)$ exhibits an isolated pole at $\zeta = -(p - q)$. The spectral functions

$$w_+(\lambda) = \frac{A}{\pi} \cdot \frac{\sqrt{\lambda - p}\Theta(\lambda - p)}{\lambda - p + q}, \; w_-(\lambda) = w_+(\lambda) + 2A\sqrt{q}\delta(\lambda - p + q) \tag{3.10}$$

differ only by the contribution from this pole. Here $\Theta(\cdot)$ is the Heaviside step function. The conductivity distributions associated with $c_\pm(\zeta)$ are

$$\mu_0\sigma_\pm(z) = \frac{A^2}{[A - (\sqrt{p} \pm \sqrt{q})z]^2[A + (\sqrt{p} \mp \sqrt{q})z]^2}. \tag{3.11}$$

They are shown in Fig. 5 and give rise to the electric field

$$E_\pm(z) \sim [A - (\sqrt{p} \pm \sqrt{q})z]^{\alpha_+}[A + (\sqrt{p} \mp \sqrt{q})z]^{\alpha_-} \tag{3.12}$$

with $\alpha_\pm = (1 \pm \sqrt{1 + \zeta/p})/2$.

3.2 Constant-phase conductivity models

In this section, the restriction $0 < \sigma(0) < \infty$ is dropped and $\sigma(0)$ is allowed to attain both bounds. As a generalization of the spectral function (1.14) of a uniform half-space, we consider for $0 < \lambda < \infty$ an inverse power law, in which spectral function $w(\lambda)$ and response function $c(\zeta)$ are related by

$$w(\lambda) = \frac{\sin(\pi\epsilon)}{\pi} \cdot \frac{A_\epsilon}{\lambda^\epsilon}, \; c(\zeta) = \frac{A_\epsilon}{\zeta^\epsilon}, \; 0 < \epsilon < 1. \tag{3.13}$$

The integral representation (1.4) converges only for the restricted range of the exponent ϵ. Obviously no moment of $w(\lambda)$ exists. The positive amplitude A_ϵ, generally depending on ϵ and of dimension m $s^{-\epsilon}$, is at our disposal. The selection in eq. (3.13) was guided by the quest for a

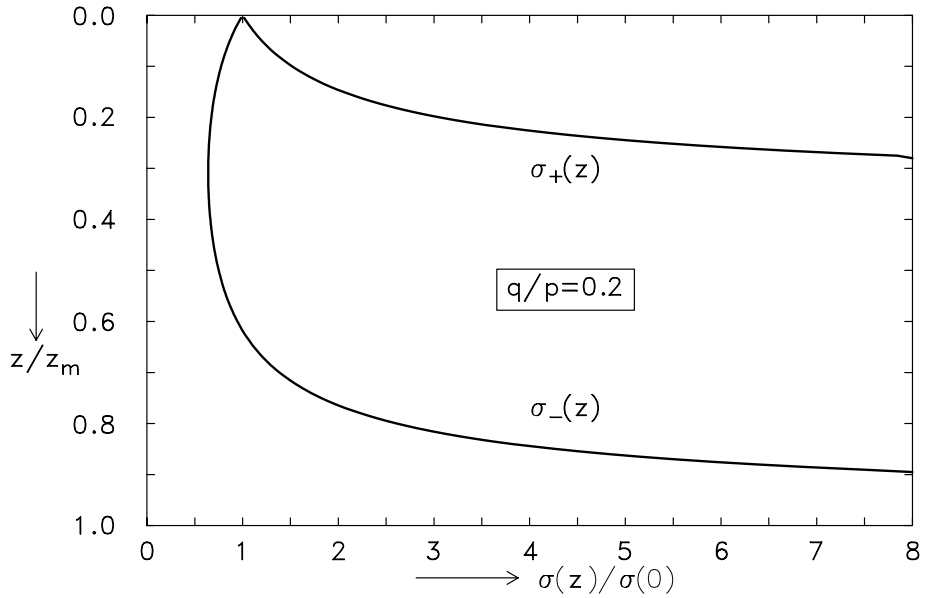

Figure 5. Conductivity distributions $\sigma_\pm(z)$ corresponding to spectral functions $w_\pm(\lambda)$ with the same continuous part and an additional spectral line of $w_-(\lambda)$. The dominating influence of this line on $\sigma_-(z)$ is obvious, because an isolated spectral line corresponds to a thin surface sheet with a perfect conductor at depth. For $z \to z_m := A/(\sqrt{p} - \sqrt{q})$, conductivity σ_- tends to infinity. The parameters are defined in the text.

simple $c(\zeta)$. The magnetotelluric response functions (apparent resistivity ϱ_a and phase φ) are

$$\varrho_a = \omega\mu_0|c|^2 = \mu_0 A_\epsilon^2 \omega^{1-2\epsilon}, \varphi = \pi/2 + \arg(c) = (\pi/2)(1-\epsilon). \tag{3.14}$$

As a particular facet, the phase is independent of frequency. Clearly, $\epsilon = 1/2$ refers to the uniform half-space. However, which conductivity profile is connected with arbitrary ϵ?

This question is answered by relating eq. (3.13) to the Jacobian spectral function (C1) with

$$\alpha = -\epsilon, \beta = 0, a = 0, b \to \infty, s_0 = \frac{A_\epsilon \sin(\pi\epsilon)}{\pi(1-\epsilon)} \cdot b^{1-\epsilon}. \tag{3.15}$$

Using eq. (C13), it is inferred that $d_n \sim s_0/b \sim 1/b^\epsilon$. Therefore $d_n \to 0$ for $b \to \infty$, i.e. the thin-sheet structure is transformed in this limit into a continuous conductor. Because a parcel of finite thickness now comprises many thin sheets, attention can be confined to eq. (C14), being the limit of eqs (C12) and (C13) for $n \gg 1$,

$$\mu_0\tau_n \simeq \frac{2\Gamma(\epsilon)n^{1-2\epsilon}}{A_\epsilon\Gamma(1-\epsilon)b^{1-\epsilon}}, \quad d_n \simeq \frac{2A_\epsilon\Gamma(1-\epsilon)n^{2\epsilon-1}}{\Gamma(\epsilon)b^\epsilon}, \tag{3.16}$$

where it was noted that $\pi/\sin(\pi\epsilon) = \Gamma(\epsilon)\Gamma(1-\epsilon)$. A conductivity $\sigma_n := \tau_n/d_n$ is assigned to a depth z_n, obtained by integrating d_n over n. Therefore,

$$\mu_0\sigma_n = \frac{\Gamma^2(\epsilon)}{A_\epsilon^2\Gamma^2(1-\epsilon)} \cdot \left(\frac{n^2}{b}\right)^{1-2\epsilon}, \quad z_n = \frac{A_\epsilon\Gamma(1-\epsilon)}{\epsilon\Gamma(\epsilon)} \cdot \left(\frac{n^2}{b}\right)^\epsilon. \tag{3.17}$$

In our application, b and n (occurring in the combination n^2/b only) independently tend to infinity. As a consequence, the parameter n^2/b can attain all positive values, with small values referring to shallow depth. Therefore, eq. (3.17) is a parameter representation of the desired conductivity profile $\sigma(z)$. In this simple case, the parameter can be eliminated to yield

$$\mu_0\sigma(z) = \left[\frac{\Gamma(\epsilon)(\epsilon z)^{1-2\epsilon}}{A_\epsilon\Gamma(1-\epsilon)}\right]^{1/\epsilon} \sim z^{-2+1/\epsilon}. \tag{3.18}$$

When approaching the surface from below, the conductivity decreases to zero for $\epsilon < 1/2$ and increases to infinity for $\epsilon > 1/2$, but remains integrable. In the first case, the limiting model for $\epsilon \to 0$ is an insulating layer over a perfect conductor at depth A_0. In the second case, a thin surface sheet with conductance $1/(\mu_0 A_1)$ is the end-member for $\epsilon \to 1$.

In view of the various limiting processes involved, it appears worthwhile to verify that $\sigma(z)$, given in eq. (3.18), in fact reproduces the response (3.13): the solution of eq. (1.2) is (Abramowitz & Stegun 1972, formula 9.1.51)

$$E(z) = \sqrt{z}\mathrm{K}_\epsilon\left[2(pz)^{1/(2\epsilon)}\right], \quad p := \frac{\epsilon\Gamma(\epsilon)\zeta^\epsilon}{A_\epsilon\Gamma(1-\epsilon)}, \tag{3.19}$$

where $\mathrm{K}_\epsilon(\cdot)$ is the modified Bessel function of the second kind and order ϵ. With the boundary values (Abramowitz & Stegun 1972, formulae 9.6.9, 9.6.26 and 9.6.6)

$$E(0) = \frac{1}{2}\Gamma(\epsilon)/\sqrt{p}, E'(0) = -\frac{1}{2\epsilon}\Gamma(1-\epsilon)\sqrt{p}, \tag{3.20}$$

the response is, according to eq. (1.3),

$$c = -\frac{E(0)}{E'(0)} = \frac{\epsilon\Gamma(\epsilon)}{p\Gamma(1-\epsilon)} = \frac{A_\epsilon}{\zeta^\epsilon}. \tag{3.21}$$

3.3 Piecewise continuous conductors including thin sheets

Stack of thin sheets over a piecewise continuous conductor. By the non-linear interaction of a finite stack of thin sheets with an underlying piecewise continuous conductor $\sigma_{\mathrm{pc}}(z)$, essential properties of the thin sheet response function, characterized by a finite number of poles, are imparted to the combined response function $c(\zeta)$: if the response function $c_{\mathrm{pc}}(\zeta)$ has a branch cut at $\zeta = -\lambda_B$, then $c(\zeta)$ can show a number of poles in $0 > \zeta > -\lambda_B$ resulting from the thin sheets. Moreover, the stack of thin sheets acts as a low-pass filter by damping $w(\lambda)$ for $\lambda \to \infty$. Consequently, now a number of moments exist, which allow all thin-sheet parameters to be resolved.

Transferring the general case to Appendix E, here only an illustrative example is considered. It consists of a thin surface sheet of conductance $\tau_0 > 0$ overlying a piecewise continuous conductor with $\sigma_{\mathrm{pc}}(z) = \sigma_0/(1-\mu_0\sigma_0 pz^2)^2$ [see eq. (3.11) with $q = 0$ and $A^2 = 1/(\mu_0\sigma_0)$]. The corresponding response function and spectral function are, following eqs (3.9) and (3.10),

$$c_{\mathrm{pc}}(\zeta) = \frac{1}{\sqrt{(\zeta+p)\mu_0\sigma_0}}, \quad w_{\mathrm{pc}}(\lambda) = \frac{\Theta(\lambda-p)}{\pi\sqrt{(\lambda-p)\mu_0\sigma_0}}, p > 0. \tag{3.22}$$

With $1/c(\zeta) = \zeta\mu_0\tau_0 + 1/c_{\mathrm{pc}}(\zeta)$ and eq. (1.11), the combined model gives

$$c(\zeta) = \frac{1}{\zeta\mu_0\tau_0 + \sqrt{(\zeta+p)\mu_0\sigma_0}}, w(\lambda) = \frac{1}{\pi} \cdot \frac{\sqrt{(\lambda-p)\mu_0\sigma_0}\Theta(\lambda-p)}{(\lambda\mu_0\tau_0)^2 + (\lambda-p)\mu_0\sigma_0} + v_1\delta(\lambda-\kappa_1) \tag{3.23}$$

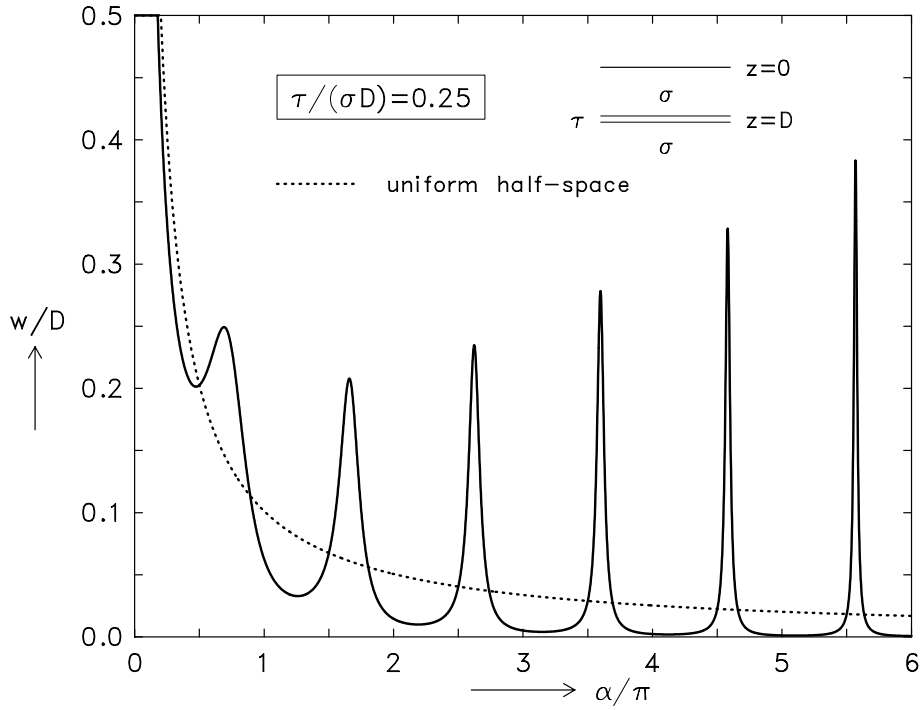

Figure 6. Spectral function $w(\lambda)$ of a single thin sheet embedded in a uniform half-space. With increasing $\alpha = \sqrt{\lambda\mu_0\sigma}\,D$ the height of the peaks increases ($\simeq\alpha_m\beta^2/\pi$) but the area under the peak decreases ($\simeq 1/\alpha_m$), where $\beta := \tau/(\sigma\ D)$ and $\alpha_m \simeq (m-1/2)\pi$ is the approximate position of the mth peak for $m \gg 1$.

with

$$v_1 = \frac{1}{\mu_0\tau_0}\cdot\frac{\alpha}{\sqrt{1+\alpha}(1+\sqrt{1+\alpha})}, \kappa_1 = \frac{2p}{1+\sqrt{1+\alpha}} < p, \alpha := 4p\mu_0\tau_0^2/\sigma_0, \tag{3.24}$$

where $\zeta = -\kappa_1$ is the pole of $c(\zeta)$. Because $w(\lambda) = \mathcal{O}(\lambda^{-3/2})$ for $\lambda \to \infty$, the zero-order moment s_0 of $w(\lambda)$ exists and yields (including the contribution from the pole) $s_0 = 1/(\mu_0\tau_0)$. It allows τ_0 to be resolved and is independent of $\sigma_{\rm pc}(z)$.

Thin sheet embedded in a piecewise continuous conductor. This model class will be illustrated by the following two simple examples only.

(i) Thin sheet of conductance τ embedded at depth $z = D$ in a uniform half-space of conductivity σ. The response

$$\frac{c(\zeta)}{D} = \frac{1}{a}\cdot\frac{1+a\beta+\coth a}{(1+a\beta)\coth a+1}, \quad a := \sqrt{\zeta\mu_0\sigma}\,D, \quad \beta := \frac{\tau}{\sigma D}, \tag{3.25}$$

gives rise to the spectral function

$$\frac{w(\lambda)}{D} = \frac{1}{\alpha\pi[1+\alpha\beta\sin(2\alpha)+\alpha^2\beta^2\cos^2\alpha]}, \quad \alpha := \sqrt{\lambda\mu_0\sigma}\,D. \tag{3.26}$$

The parameter β is the conductance ratio of thin sheet to overburden. The resulting spectral function is displayed in Fig. 6. For $D > 0$, no moment exists: $w(\lambda)$ oscillates around the uniform half-space spectral function (dotted line) and shows peaks near $\alpha = \alpha_m \simeq (m-1/2)\pi$, $m = 1, 2, 3, \ldots$. The peaks get more pronounced with increasing λ and β, and thus $w(\lambda)$ resembles more and more the spectral function (3.3) of a uniform layer overlying a perfect conductor. For $m \gg 1$, the area under the peaks approaches $1/\alpha_m \sim 1/m$, which underlines that not even the zero-order moment exists.

(ii) Periodic sequence of thin sheets of conductance τ embedded at depth $z = nD$, $n = 1, 2, 3, \ldots$, in a uniform half-space of conductivity σ. The periodicity condition yields the response

$$\frac{c(\zeta)}{D} = \frac{1}{a}\cdot\frac{a\beta/2+\sqrt{1+a\beta\coth a+(a\beta/2)^2}}{1+a\beta\coth a}. \tag{3.27}$$

Let $R := 1+\alpha\beta\cot\alpha-(\alpha\beta/2)^2$. Then $c(\zeta)$ is associated with the spectral function

$$\frac{w(\lambda)}{D} = \frac{1}{\alpha\pi}\cdot\frac{\sqrt{R}\Theta(R)}{1+\alpha\beta\cot\alpha}+\sum_{m=1}^{\infty}\frac{\beta^2\alpha_m\delta(\alpha-\alpha_m)}{\beta+\sec^2\alpha_m}, \tag{3.28}$$

where $\Theta(\cdot)$ is again the Heaviside step function and α_m is the mth positive solution of $1+\alpha\beta\cot\alpha = 0$ with $\alpha_m \simeq (m-1/2)\pi$, $\sec\alpha_m \simeq (-1)^m\beta\alpha_m$ for $m \gg 1$. As in the previous example, in this limit the amplitude of $\delta(\alpha-\alpha_m)$ is $1/\alpha_m$ and therefore no moment exists. This asymptotic behaviour is also seen in Fig. 7, which displays $w(\lambda)/D$. Because $\alpha_m\delta(\alpha-\alpha_m) = 2\lambda_m\delta(\lambda-\lambda_m)$, in the λ representation the amplitudes tend to the constant value $w_m \simeq 2/(\mu_0\sigma\ D)$.

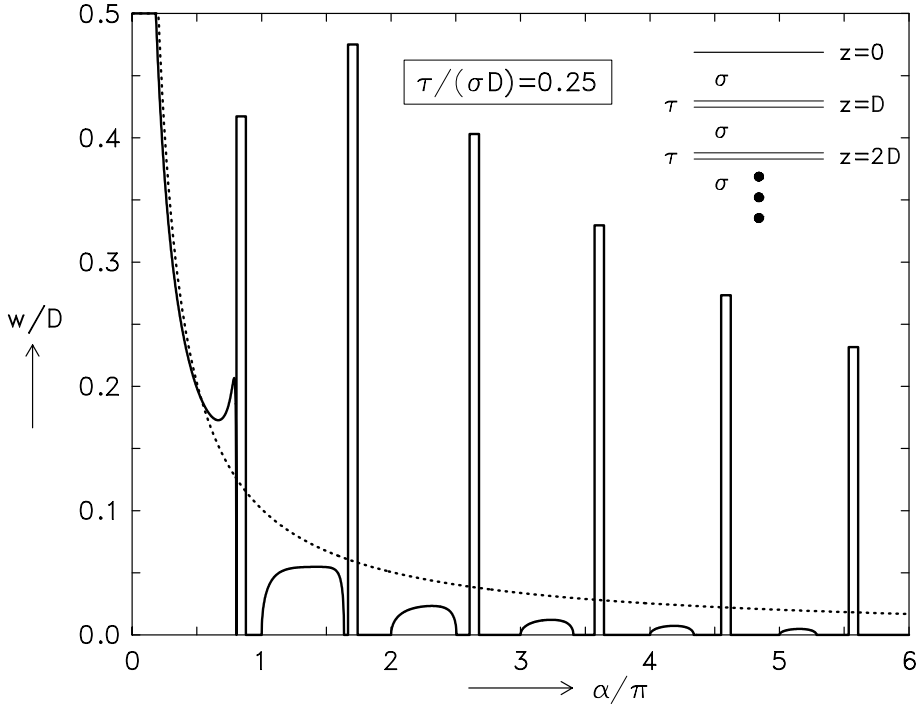

Figure 7. Spectral function $w(\lambda)$ of a periodic sequence of thin sheets embedded into a uniform half-space. It results in an infinite number of continuous spectral sections separated by discrete spectral lines. These lines are displayed by rectangular boxes of equal width, with an area corresponding to the strength of the line.

3.4 Inversion of the spectral function for piecewise continuous conductors

In the case of thin sheets, the sheet parameters could be inferred from the spectral function by the numerical algorithm described in Section 2.2. For piecewise continuous conductors, the situation is more complicated. At least in the case that $\sigma(z)$ has no discontinuities at all, the various Gel' fand–Levitan type techniques will serve for this purpose (Weidelt 1972; Whittall & Oldenburg 1986, 1992). Without readdressing the topic in detail, only a short description is given.

The unstable determination of the spectral function $w(\lambda)$ from experimental data is the most difficult part of the inverse problem. However, if $w(\lambda)$ is assumed known, the inverse problem is reduced to a stable (linear) Fredholm integral equation of the second kind, in which the kernel is derived from $w(\lambda)$. Let $0 < \sigma(0) < \infty$, $\mu := \sqrt{\lambda\mu_0\sigma(0)}$ and $\tilde{w}(\mu) := w(\lambda)$. Then $\tilde{w}(\mu) \to 1/(\pi\mu)$ for $\mu \to \infty$ and the kernel of the integral equation is constructed from

$$B(x) := \begin{cases} 0, & x < 0, \\ (1/\pi)\int_0^\infty [1 - \pi\mu\tilde{w}(\mu)]\cos(\mu x)\,d\mu, & x \geq 0, \end{cases} \tag{3.29}$$

where x has the dimension of a length (a distorted depth coordinate). The kernels of the linear integral equations are $K(x|y) = B(x + y) + B(x - y)$ in the Gel' fand–Levitan method and $K(x|y) = B(|x - y|)$ in the Gopinath–Sondhi technique. The latter technique is applicable even to a discontinuous $\sigma(z)$. For further details, see the references given above.

4 CONCLUDING REMARKS

This paper investigates for the first time in some detail the question how in 1-D magnetotellurics the conductivity structure $\sigma(z)$ is mapped onto the structure of the corresponding spectral function $w(\lambda)$. A gross summary is given in Table 1. It classifies the conductivity structures according to obvious properties of the spectral function such as continuous and discrete parts and how many moments exist. The term 'strong parameter variation' is not well defined. With reference to the end of Appendix B, it means, loosely speaking, that for $n \gg 1$ asymptotically the limits 0 or ∞ are attained either for the product $\tau_n d_{n+1}$ or for the ratio of parameters of adjacent sheets.

Appropriate mathematical tools for the treatment of thin-sheet structures are CFs, orthogonal polynomials, Hankel determinants and second-order difference equations, which show an intimate relationship and allow one to see the $w(\lambda)$–$\sigma(z)$ correspondence under different aspects (Sections 2.1–2.3 and the Appendices A and B). For instance, the three-term recurrence relations (A3) for CFs, eq. (2.7) for orthogonal polynomials and eq. (B3) for second-order difference equations turn out to be different views of the same object.

Table 1 is incomplete as far as thin sheets embedded in piecewise continuous conductors are concerned. For these conductivities, no moment exists, but the nature of the spectrum found in the examples at the end of Section 3.3 (a continuous spectrum or an infinite sequence

Table 1. First classification of conductivity structures according to how many moments of $w(\lambda)$ exist and the nature of its spectrum. Examples for a strong parameter variation are given at the end of Appendix B.

Number of moments	Nature of the spectrum	
	Continuous sections with some discrete lines	Completely discrete
All moments exist	Infinite sequence of thin sheets	Finite sequence of thin sheets or infinite sequence of thin sheets with a strong parameter variation
A few moments exist	Thin sheets over a piecewise continuous conductor with $I = \infty$	Thin sheets over a piecewise continuous conductor with $I < \infty$
No moment exists	Piecewise continuous conductor with $I = \infty$	Piecewise continuous conductor with $I < \infty$

Abbreviation: $I := \int_0^{z_m} \sqrt{\sigma(z)}\, dz$, where $z_m = \infty$ or the depth of a perfect conductor.

of continuous sections, separated by a single spectral line) does not fit into the scheme of Table 1; for these structures an extension of the table is required.

No systematic treatment of the $w(\lambda)$–$\sigma(z)$ relation for piecewise conductors has been attempted. The examples in Section 3 have been selected mostly for an informative illustration rather than for a systematic coverage of all aspects.

ACKNOWLEDGMENTS

My particular thanks go to the reviewers Kathy Whaler and Gary Egbert for their thoughtful criticism, which (hopefully) has improved the readability of the paper. I am deeply indebted to Jet Wimp for his efficient help in evaluating certain Hankel determinants. This help in an early stage of the work has opened the door to a more coherent treatment of the topic.

REFERENCES

Abramowitz, M. & Stegun, I.A., 1972. *Handbook of mathematical functions,* Dover Publications, New York.

Achieser (Akhiezer), N.I. & Glasmann (Glazman), I.M., 1977. *Theorie der linearen Operatoren im Hilbert-Raum,* Harri Deutsch, Thun & Frankfurt/Main.

Erdélyi, A., Magnus, W., Oberhettinger, F. & Tricomi, F.G., 1953. *Higher transcendental functions*, Vol. 2, McGraw-Hill Book Co., New York.

Gradshteyn, I.S. & Ryzhik, I.M., 1980. *Table of integrals series and products,* Academic Press, New York.

Grommer, J., 1914. Ganze transzendente Funktionen mit lauter reellen Nullstellen, *Journal für die reine und angewandte Mathematik,* **144,** 114–165.

Hinton, D.B. & Lewis, R.T., 1978. Spectral analysis of second order difference equations, *J. Mathematical Analysis and Applications,* **63,** 421–438.

Markoff (Markov), A., 1895. Deux démonstrations de la convergence des certaines fractions continues, *Acta Mathematica,* **19,** 93–104.

Morse, P.M. & Feshbach, H., 1953. *Methods of theoretical physics,* Vol. 1, McGraw-Hill, New York.

Parker, R.L., 1980. The inverse problem of electromagnetic induction: existence and construction of solutions based on incomplete data, *J. geophys. Res.,* **85,** 4421–4428.

Parker, R.L. & Whaler, K.A., 1981. Numerical methods for establishing solutions to the inverse problem of electromagnetic induction, *J. geophys. Res.,* **86,** 9574–9584.

Perron, O., 1913. *Die Lehre von den Kettenbrüchen*, Verlag von B.G. Teubner, Leipzig & Berlin.

Pólya, G. & Szegö, G., 1971. *Aufgaben und Lehrsätze aus der Analysis II,* 4th edn, Heidelberger Taschenbücher, Vol. 74, Springer-Verlag, Berlin.

Schmucker, U., 1970. Anomalies of geomagnetic variations in the southwestern United States, *Bull. Scripps Inst. Oceanogr.,* **13,** 1–165.

Shohat, J.A. & Tamarkin, J.D., 1943. *The problem of moments*, Mathematical Surveys, Vol. 1, American Mathematical Society, Providence, RI.

Szegö, G., 1975. *Orthogonal polynomials,* 4th edn, American Mathematical Society Colloquium Publications, Vol. 23, American Mathematical Society, Providence, RI.

Tikhonov, A.N., 1965. Mathematical basis of the theory of electromagnetic soundings, *USSR Comput. Math. and Math. Phys.,* **5,** 207–211.

Wall, H.S., 1948. *Analytic theory of continued fractions*, Van Nostrand, Princeton, NJ.

Weidelt, P., 1972. The inverse problem of geomagnetic induction, *Z. f. Geophysik,* **38,** 257–289.

Weidelt, P., 1986. Discrete frequency inequalities for magnetotelluric impedances of one-dimensional conductors, *J. Geophys.,* **59,** 171–176.

Whittall, K.P. & Oldenburg, D.W., 1986. Inversion of magnetotelluric data using a practical inverse scattering formulation, *Geophysics,* **51,** 383–395.

Whittall, K.P. & Oldenburg, D.W., 1992. *Inversion of magnetotelluric data for a one-dimensional conductivity, Geophysical Monograph Series,* Vol. 5, Society of Exploration Geophysicists, Tulsa, OK.

Wimp, J., 2000. Hankel determinants of some polynomials arising in combinatorial analysis, *Numerical Algorithms,* **24,** 179–193.

Wouk, A., 1953. Difference equations and J-matrices, *Duke Math. J.,* **20,** 141–159.

Yee, E. & Paulson, K.V., 1988a. Properties of the c-response function for conductivity distributions of class $\overline{S}^+$, *Geophys. J.,* **93,** 265–278.

Yee, E. & Paulson, K.V., 1988b. Necessary and sufficient conditions for the existence of a solution to the one-dimensional magnetotelluric inverse problem, *Geophys. J.,* **93,** 279–293.

APPENDIX A: DIRECT EXPRESSION OF THE SHEET PARAMETERS IN TERMS OF THE MOMENTS

In Section 2.3, the relationship (2.32) and (2.33) between the moments s_k and the sheet parameters τ_n and d_n was derived via orthogonal polynomials. The alternative derivation of this appendix can be obtained from results presented by Perron (1913, § 58 and § 67) after a number of transformations. With a loose reference to this source, we will give a short derivation directly related to the pertinent CF (2.20). Let

$$c^{(m)}(\zeta) := \frac{A_m(\zeta)}{B_m(\zeta)} \tag{A1}$$

be the mth order approximant of $c(\zeta)$ in its representation by the CF (2.20). With the starting values

$$A_0 = 0, \quad B_0 = 1, \quad A_1 = 1, \quad B_1 = \mu_0\tau_0\zeta, \tag{A2}$$

$A_m(\zeta)$ and $B_m(\zeta)$ are for $n = 1, 2, 3, \ldots$ recursively obtained from

$$X_{2n} = d_n X_{2n-1} + X_{2n-2}, \quad X_{2n+1} = \mu_0\tau_n\zeta X_{2n} + X_{2n-1}, \tag{A3}$$

where $X_m := A_m$ or $X_m := B_m$ (e.g. Wall 1948, p. 15). By induction it is inferred that

$$A_{2n}(\zeta) = \sum_{\ell=0}^{n-1} a_{2n,\ell}\zeta^\ell, \quad B_{2n}(\zeta) = 1 + \sum_{\ell=1}^{n} b_{2n,\ell}\zeta^\ell, \tag{A4}$$

$$A_{2n+1}(\zeta) = 1 + \sum_{\ell=1}^{n} a_{2n+1,\ell}\zeta^\ell, \quad B_{2n+1}(\zeta) = \sum_{\ell=1}^{n+1} b_{2n+1,\ell}\zeta^\ell, \tag{A5}$$

where in particular

$$b_{2n,n} = \prod_{k=1}^{n}(\mu_0\tau_{k-1}d_k), \quad b_{2n+1,n+1} = \mu_0\tau_n\prod_{k=1}^{n}(\mu_0\tau_{k-1}d_k), \tag{A6}$$

implying

$$\mu_0\tau_n = b_{2n+1,n+1}/b_{2n,n}, \quad d_{n+1} = b_{2n+2,n+1}/b_{2n+1,n+1}. \tag{A7}$$

Eq. (A7) shows that for the computation of τ_n and d_n only the coefficients (A6) have to be determined. Again by induction it is found (e.g. Wall 1948, p. 16) that

$$c^{(m+1)}(\zeta) - c^{(m)}(\zeta) = \frac{(-1)^m}{B_m(\zeta)B_{m+1}(\zeta)}, \tag{A8}$$

which, according to eqs (A4) and (A5), is $\mathcal{O}(1/\zeta^{m+1})$ for $|\zeta| \to \infty$. After expanding the kernel $1/(\lambda + \zeta)$ in the integral representation (1.4) of $c(\zeta)$ in powers of $1/\zeta$, $|\zeta| \to \infty$, we obtain a representation of $c(\zeta)$ in terms of its moments,

$$c(\zeta) = \sum_{k=0}^{\infty} \frac{(-1)^k s_k}{\zeta^{k+1}}. \tag{A9}$$

If $w(\lambda) = 0$ for $\lambda > b$, $b < \infty$, this expansion is convergent for $|\zeta| > b$, otherwise it is valid only asymptotically. Because $c^{(m)}(\zeta)$ and $c^{(m+1)}(\zeta)$ agree in powers of $1/\zeta$ less than $m + 1$, it can be concluded that $c^{(m)}$ reproduces the first m terms of the expansion (A9), i.e.

$$c^{(m)}(\zeta) = \sum_{k=0}^{m-1} \frac{(-1)^k s_k}{\zeta^{k+1}} + \sum_{k=m}^{\infty} \frac{g_{mk}}{\zeta^{k+1}}, \tag{A10}$$

where only the coefficients g_{mk} of the second sum depend on the order m of approximation. Multiplication of eq. (A10) with $B_m(\zeta)$ yields

$$A_m(\zeta) = B_m(\zeta)\cdot\sum_{k=0}^{m-1} \frac{(-1)^k s_k}{\zeta^{k+1}} + B_m(\zeta)\cdot\sum_{k=m}^{\infty} \frac{g_{mk}}{\zeta^{k+1}}. \tag{A11}$$

First, let $m = 2n$ and compare the coefficients of the powers $(1/\zeta)^j$, $j = 1, \ldots, n$. With reference to eq. (A5), we obtain the n equations

$$\sum_{k=0}^{n-1}(-1)^{j+k} s_{j+k} b_{2n,k+1} = (-1)^j s_{j-1}, \quad j = 1, \ldots, n. \tag{A12}$$

The range of j is chosen in such a way that the coefficients $a_{m\ell}$ and g_{mk} are not involved. The right-hand side results from the term $b_{2n,0} = 1$ in eq. (A4). The solution of this set of equations for $b_{2n,n}$ gives, with $\Delta_n(i)$ defined in eq. (2.30),

$$b_{2n,n} = \frac{\Delta_n(0)}{\Delta_n(1)}, \tag{A13}$$

using

$$\det\left[(-1)^{i+j+k} s_{i+j+k}\right]_{j,k=0,\ldots,n-1} = (-1)^{n\cdot i}\det[s_{i+j+k}]_{j,k=0,\ldots,n-1}. \tag{A14}$$

Next consider eq. (A11) with $m = 2n + 1$. A comparison of the coefficients of $(1/\zeta)^j$, $j = 0, \ldots, n$, yields with reference to eq. (A5) the $n + 1$ equations

$$\sum_{k=0}^{n}(-1)^{j+k} s_{j+k} b_{2n+1,k+1} = \delta_{0j}, \quad j = 0, \ldots, n, \tag{A15}$$

where δ_{mn} is the Kronecker symbol. The right-hand side originates from the term $a_{2n+1,0} = 1$ in eq. (A5). Solving for $b_{2n+1,n+1}$, we obtain

$$b_{2n+1,n+1} = \frac{\Delta_n(1)}{\Delta_{n+1}(0)}. \tag{A16}$$

Eqs (A7), (A13) and (A16) then yield the desired expressions (2.32) and (2.33) of the sheet parameters in terms of the moments.

APPENDIX B: COMPUTATION OF $W(\lambda)$ FOR GIVEN THIN-SHEET PARAMETERS

This appendix sketches the solution of the forward problem, i.e. the determination of $w(\lambda)$ from the sheet parameters. First, a finite stack of N thin sheets with conductances τ_n at $z = z_n$, $0 \le n \le N-1$, is assumed (see Fig. 2). The sequence is terminated with $\tau_N = \infty$ at $z = z_N$. Moreover, $z_0 = 0$, $d_{n+1} = z_{n+1} - z_n$. Then the eigenvalue problem (1.5) reads

$$e'(z_n^+) - e'(z_n^-) = -\lambda\mu_0\tau_n e(z_n),\ 0 \le n \le N-1 \tag{B1}$$

with $e'(z_n^-) = [e(z_n) - e(z_{n-1})]/d_n$, $e'(z_n^+) = [e(z_{n+1}) - e(z_n)]/d_{n+1}$ and the boundary conditions $e'(z_0^-) = 0$, $e(z_N) = 0$. With

$$f_n := \sqrt{\mu_0\tau_n}e(z_n),\ \mathbf{f} := (f_0, f_1, \ldots, f_{N-1})^T \tag{B2}$$

it reduces to

$$\mathbf{J}_N\mathbf{f} = \lambda\mathbf{f}, \tag{B3}$$

where $\mathbf{J}_N$ is the N-dimensional symmetric tridiagonal matrix (Jacobi matrix)

$$\mathbf{J}_N = \begin{pmatrix} \alpha_0 & \beta_1 & & & & \\ \beta_1 & \alpha_1 & \beta_2 & & & \\ & & \cdot & \cdot & & \\ & & \cdot & \cdot & & \\ & & & \beta_{N-2} & \alpha_{N-2} & \beta_{N-1} \\ & & & & \beta_{N-1} & \alpha_{N-1} \end{pmatrix} \tag{B4}$$

with

$$\alpha_0 := \frac{1}{\mu_0\tau_0 d_1},\ \alpha_n := \frac{1}{\mu_0\tau_n}\cdot\left(\frac{1}{d_n} + \frac{1}{d_{n+1}}\right),\ \beta_n := -\frac{1}{\mu_0\sqrt{\tau_{n-1}\tau_n}d_n},\ 1 \le n \le N-1, \tag{B5}$$

implying that the principal subdeterminants

$$\det\mathbf{J}_n = 1/\prod_{m=0}^{n-1}(\mu_0\tau_m d_{m+1}),\quad 1 \le n \le N, \tag{B6}$$

are positive. Therefore, $\mathbf{J}_N$ is positive definite. Hence, for finite τ_n, d_n and N, all eigenvalues λ_m, $1 \le m \le N$, are positive. Let $\mathbf{f}_m$ be the normalized eigenvectors, $\mathbf{f}_m^T\mathbf{f}_j = \delta_{mj}$. Then $\mathbf{F} := (\mathbf{f}_1, \mathbf{f}_2, \ldots, \mathbf{f}_N)$ with the entries F_{nm} is an orthogonal $N \times N$ matrix. Let the polarity of $\mathbf{f}_m$ be fixed by $F_{0m} > 0$. Conventional methods provide the expansion of the solution of eq. (1.2) in terms of $F_{nm} =: \sqrt{\mu_0\tau_n}e_m(z_n)$,

$$E(z_n, \zeta) = -\frac{E'(0^-, \zeta)}{\mu_0\sqrt{\tau_0\tau_n}}\sum_{m=1}^{N}\frac{F_{0m}F_{nm}}{\lambda_m + \zeta} = -E'(0^-, \zeta)\sum_{m=1}^{N}\frac{e_m(0)e_m(z_n)}{\lambda_m + \zeta}, \tag{B7}$$

and in particular, using eq. (1.3) and $s_0 = 1/(\mu_0\tau_0)$,

$$c(\zeta) = \sum_{m=1}^{N}\frac{w_m}{\lambda_m + \zeta}\quad \text{with}\quad w_m = s_0F_{0m}^2 = e_m^2(0). \tag{B8}$$

This solves the forward problem for finite N.

Whereas the orthogonality of the columns of $\mathbf{F}$ expresses the orthogonality of the eigenvectors, the orthogonality of the rows of $\mathbf{F}$ is associated with the orthogonality of the orthogonal polynomials $p_n(\lambda)$. Let $p_n(\lambda_m) := F_{nm}/\sqrt{w_m}$. Then

$$\sum_{m=1}^{N}F_{nm}F_{km} = \delta_{nk} = \sum_{m=1}^{N}w_m p_n(\lambda_m)p_k(\lambda_m) = (p_n, p_k), \tag{B9}$$

where the normalization (2.24) has been adopted. It implies $p_0(\lambda_m) = 1/\sqrt{s_0}$. Row $(n+1)$ of eq. (B3) reads for $\mathbf{f} = \mathbf{f}_m$ (after division by $\sqrt{w_m}$)

$$\beta_n p_{n-1}(\lambda_m) + \alpha_n p_n(\lambda_m) + \beta_{n+1}p_{n+1}(\lambda_m) = \lambda_m p_n(\lambda_m), \tag{B10}$$

which is the three-term recurrence relation (2.25). In contrast to $\beta_j > 0$ assumed there, the parameters β_j are negative here. This difference changes only the polarity of the polynomials of odd degree, such that now $p_n(0) > 0$ for all n. For given τ_n and d_n, the polynomials $p_n(\lambda)$ can be calculated via eqs (B5) and (B10).

For $N \to \infty$, the discrete spectral lines obtained for finite N will either cluster to one or more continuous sections of finite or infinite support (with a few discrete lines subsisting) or they will remain discrete, either with λ_∞ as a finite point of accumulation or increasing to $+\infty$.

Of particular interest is an investigation of the conditions under which the spectrum remains discrete for $N \to \infty$. Although it appears to be difficult to formulate conditions for the coefficients α_n and β_n, which are both necessary and sufficient, at least some sufficient conditions can be found in the literature. The spectrum remains discrete if for $n \to \infty$ one of the following conditions applies.

(i) $\alpha_n \to \lambda_\infty \geq 0$, $\beta_n \to 0$ (after Achieser & Glasmann 1977, p. 80).
Examples:

(a) $\tau_n \sim n!, d_{n+1} \sim 1/n!, \alpha_n \sim (1 + 1/n) \to \lambda_\infty > 0, \beta_n \sim 1/\sqrt{n} \to 0$;
(b) $\tau_n \sim q_\tau^n, d_n \sim q_d^n, q_\tau q_d > 1, \alpha_n \to \lambda_\infty = 0, \beta_n \to 0$.

Achieser & Glasmann consider only the case $\lambda_\infty = 0$, but $\lambda_\infty > 0$ is a simple extension of it.
(ii) $\alpha_n + \beta_n + \beta_{n+1} \to +\infty$ (Hinton & Lewis 1978 p. 431).
Examples:

(a) $\tau_n \sim 1/n!, d_{n+1} \sim n!, \alpha_n + \beta_n + \beta_{n+1} \sim (n + 1 - \sqrt{n} - \sqrt{n+1}) \to +\infty$
[this parameter set is a special case of eq. (2.93) and gives rise to the Charlier polynomials];
(b) $\tau_n \sim q_\tau^n, d_n \sim q_d^n, q_d < q_\tau q_d < 1$ or $1/q_d < q_\tau q_d < 1, \alpha_n + \beta_n + \beta_{n+1} \sim (1 - q_\tau)(q_\tau q_d^2 - 1)/(q_\tau q_d)^n \to +\infty$.

In the examples, $\sim$ denotes proportionality with a positive constant independent of n. In case (i) the discrete eigenvalues accumulate at the finite value λ_∞, in case (ii) the discrete eigenvalues tend to infinity.

APPENDIX C: THIN-SHEET MODELS GENERATED BY JACOBI POLYNOMIALS

The Legendre and Chebyshev spectral functions (*cf.* Section 2.4.1) are members of the great family of Jacobi spectral functions

$$w(\lambda) = \frac{s_0(\lambda - a)^\alpha (b - \lambda)^\beta}{(b - a)^{\alpha+\beta+1} B(\alpha + 1, \beta + 1)}, \alpha > -1, \beta > -1, 0 \leq a < \lambda < b, \tag{C1}$$

where $B(x, y) := \Gamma(x)\Gamma(y)/\Gamma(x + y)$ is Euler's Beta function. Fig. C1 shows a normalized version of $w(\lambda)$ for the symmetric choice $\alpha = \beta$. Legendre polynomials result from $\alpha = \beta = 0$, Chebyshev polynomials from $\alpha = \beta = -1/2$. The response function is (Gradshteyn & Ryzhik 1980, integral 3.228.3)

$$c(\zeta) = \frac{s_0}{b + \zeta}\, {}_2F_1(1, \beta + 1; \alpha + \beta + 2; z), z := (b - a)/(b + \zeta), \tag{C2}$$

where ${}_2F_1$ is the hypergeometric function (e.g. Abramowitz & Stegun 1972, chapter 15), which converges inside the unit circle $|z| = 1$. Because $\Re\zeta = 0$, on the unit circle only the point $z = 1$ can be reached (for $a = \zeta = 0$). Here, ${}_2F_1$ diverges for $-1 < \alpha \leq 0$. In this case,

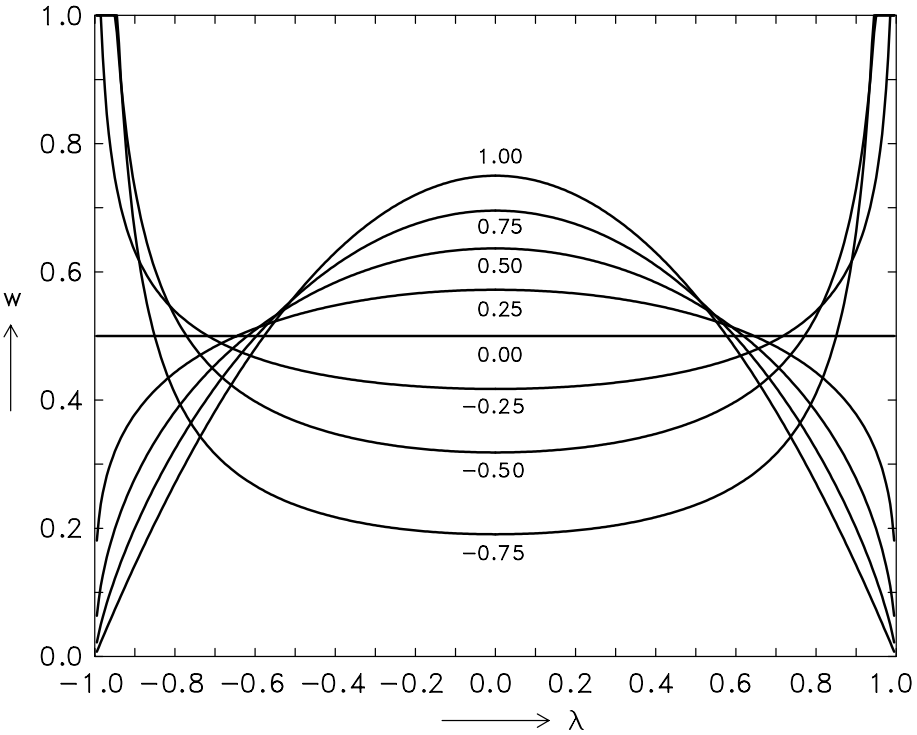

Figure C1. Normalized Jacobi weight functions $w(\lambda)$ with $a = -1$, $b = +1$ and $s_0 = 1$. Shown are only symmetric functions with $\alpha = \beta$ (curve parameter). In addition, there are asymmetric weight functions with $\alpha \neq \beta$, e.g. the periodic model (C15) with $\alpha = -0.5$, $\beta = +0.5$.

$c(0) = \infty$ means that a terminating perfect conductor is missing. Convenient for numerical evaluation is the power series

$$c(\zeta) = \frac{s_0}{b+\zeta} \cdot \sum_{m=0}^{\infty} \frac{(\beta+1)_m}{(\alpha+\beta+2)_m} \left(\frac{b-a}{b+\zeta}\right)^m \tag{C3}$$

with the Pochhammer symbol

$$(x)_m := x \cdot (x+1) \cdot (x+2) \ldots (x+m-1) = \Gamma(x+m)/\Gamma(x), \tag{C4}$$

implying in particular $(x)_0 = 1$, $(1)_m = m!$. Associated with eq. (C1) are the Jacobi polynomials

$$p_n(\lambda) = P_n^{(\beta,\alpha)}\left(\frac{2\lambda - a - b}{b-a}\right) \tag{C5}$$

with

$$p_n(0) = P_n^{(\beta,\alpha)}(-u) = (-1)^n P_n^{(\alpha,\beta)}(u), \quad u := (b+a)/(b-a) \geq 1, \tag{C6}$$

where the transition from $-u$ to $+u$ requires the exchange of α and β. An explicit representation is

$$P_n^{(\alpha,\beta)}(u) = \frac{1}{2^n} \sum_{m=0}^{n} \binom{n+\alpha}{m} \binom{n+\beta}{n-m} (u-1)^{n-m} (u+1)^m. \tag{C7}$$

With the polynomial parameters

$$h_n = \frac{(n+\alpha+\beta+1)(\alpha+1)_n(\beta+1)_n s_0}{(2n+\alpha+\beta+1)(\alpha+\beta+2)_n n!}, \tag{C8}$$

$$\frac{k_{n+1}}{k_n} = \frac{2}{b-a} \cdot \frac{(2n+\alpha+\beta+1)(2n+\alpha+\beta+2)}{2(n+1)(n+\alpha+\beta+1)}, \tag{C9}$$

we obtain from eqs (2.5) and (2.6)

$$\mu_0 \tau_n = \left[P_n^{(\alpha,\beta)}(u)\right]^2 / h_n, n \geq 0, \tag{C10}$$

$$d_{n+1} = \frac{k_{n+1} h_n}{k_n P_n^{(\alpha,\beta)}(u) P_{n+1}^{(\alpha,\beta)}(u)}, n \geq 0. \tag{C11}$$

With $P_n^{(\alpha,\beta)}(1) = (\alpha+1)_n/n!$, the resulting simplification for $a = 0$ is

$$\mu_0 \tau_n = \frac{(2n+\alpha+\beta+1)(\alpha+1)_n(\alpha+\beta+2)_n}{(n+\alpha+\beta+1)(\beta+1)_n n! s_0}, n \geq 0, \tag{C12}$$

$$d_{n+1} = \frac{(2n+\alpha+\beta+2)(\beta+1)_n n!}{(\alpha+\beta+2)_n(\alpha+1)_{n+1}} \cdot \frac{s_0}{b}, n \geq 0. \tag{C13}$$

Asymptotically for $a = 0$ and $n \gg 1$,

$$\mu_0 \tau_n \simeq \frac{B(\alpha+1, \beta+1)}{\Gamma^2(\alpha+1)} \cdot \frac{2n^{2\alpha+1}}{s_0}, \quad d_{n+1} \simeq \frac{\Gamma^2(\alpha+1)}{B(\alpha+1,\beta+1)} \cdot \frac{2s_0}{bn^{2\alpha+1}}. \tag{C14}$$

The exponents $\alpha = -1/2$, $\beta = +1/2$ yield the completely periodic model $\mu_0 \tau_n = 1/s_0$, $d_{n+1} = 4s_0/b$, $n \geq 0$ with the response function

$$c(\zeta) = \frac{2s_0}{\zeta + \sqrt{\zeta(b+\zeta)}}. \tag{C15}$$

This result follows also from eq. (2.21) with $c_n = c_{n+1} =: c$. Other classical orthogonal polynomials contained in eq. (C5) are the Chebyshev polynomials of the second kind ($\alpha = \beta = 1/2$) and the Gegenbauer polynomials ($\alpha = \beta =: \gamma - 1/2$, $\gamma > -1/2$).

APPENDIX D: DISCRETE LEGENDRE POLYNOMIALS

The polynomials $\Pi_n(x|N) =: \Pi_n(x)$, $0 \leq n \leq N-1$, are polynomials of degree n in x, which are orthogonal with respect to summation over the N equidistant abscissae

$$x_m = 2m/(N-1) - 1, 0 \leq m \leq N-1, \tag{D1}$$

with $x_0 = -1$, $x_{N-1} = +1$. The standardization $\Pi_n(1) = 1$ leads to the orthogonality relation

$$\frac{1}{N} \sum_{m=0}^{N-1} \Pi_j(x_m) \Pi_n(x_m) = \frac{\delta_{jn}}{2n+1} \cdot \prod_{m=0}^{n} \frac{N+m}{N-m}. \tag{D2}$$

$\Pi_n(x)$ is easily obtained from the recurrence relation

$$(n+1)(N-n-1)\Pi_{n+1} - (2n+1)(N-1)x\Pi_n + n(N+n)\Pi_{n-1} = 0, 1 \leq n \leq N-2, \tag{D3}$$

starting with $\Pi_0 = 1$, $\Pi_1 = x$. The subsequent polynomials are

$$\Pi_2 = \frac{3(N-1)x^2 - N - 1}{2(N-2)}, \Pi_3 = \frac{x[5(N-1)^2x^2 - 3N^2 + 7]}{2(N-2)(N-3)}. \tag{D4}$$

The relation between $\Pi_n(x|N)$ and the Legendre polynomial $P_n(x)$ is

$$\lim_{N\to\infty} \Pi_n(x|N) = P_n(x). \tag{D5}$$

From eq. (D3) follows the limit, a result required in eq. (2.89),

$$\lim_{n\to N}(N-n)\Pi_n(x) = \frac{(2N-1)(N-1)}{N}[x\Pi_{N-1}(x) - \Pi_{N-2}(x)]. \tag{D6}$$

The present standardization establishes a close relationship between $\Pi_n(x)$ and $P_n(x)$ in eq. (D5). With a different normalization, these polynomials (sometimes also called Chebyshev polynomials) are treated by Erdélyi et al. (1953, p. 223) and Szegö (1975, p. 33).

APPENDIX E: STACK OF THIN SHEETS OVER A PIECEWISE CONTINUOUS CONDUCTOR

As a generalization of the introductory example of Section 3.3, it is now assumed that the overlying conductivity structure consists of N thin sheets with conductances τ_n and separations d_{n+1}, $n = 0, \ldots, N-1$. Here, $d_N \geq 0$ is the separation between the last conducting sheet τ_{N-1} and a piecewise continuous conductivity profile $\sigma_{\rm pc}(z)$ starting at $z = z_N$. Let the response function and spectral function at $z = z_N$ be given by $c_{\rm pc}(\zeta)$ and $w_{\rm pc}(\lambda)$. The corresponding surface response can be obtained by using the recursion relation (A3) with the only modification that now

$$X_{2N} = (d_N + c_{\rm pc})X_{2N-1} + X_{2N-2},\ X_m = A_m \text{ or } B_m. \tag{E1}$$

Then eq. (A1) yields

$$c(\zeta) = \frac{A_{2N}(\zeta)}{B_{2N}(\zeta)}. \tag{E2}$$

If ζ is real, both X_{2N-1} and X_{2N-2} are real too. The two cases (i) $I < \infty$ and (ii) $I = \infty$, distinguished in Section 3.1, require different treatments.

(i) $I < \infty$: then

$$c_{\rm pc}(\zeta) = \sum_{m=1}^{\infty} \frac{w_m}{\zeta + \lambda_m}, \quad w_m > 0, \quad \lambda_m \geq 0. \tag{E3}$$

Assuming first that $B_{2N-1}(-\lambda_m) \neq 0$ for all m, the poles λ_m of $c_{\rm pc}(\zeta)$ differ from the poles κ_n of $c(\zeta)$, the latter being the solutions of $B_{2N}(\zeta) = 0$. Therefore,

$$w(\lambda) = \sum_{n=1}^{\infty} v_n \delta(\lambda - \kappa_n), \quad v_n > 0, \quad \kappa_n \geq 0, \tag{E4}$$

with $v_n = A_{2N}(-\kappa_n)/B'_{2N}(-\kappa_n)$. After performing the differentiation and replacing $d_N + c_{\rm pc}(-\kappa_n)$ by $-B_{2N-2}(-\kappa_n)/B_{2N-1}(-\kappa_n)$, we obtain (omitting the argument $\zeta = -\kappa_n$ throughout)

$$\begin{aligned}\frac{1}{v_n} &= -B^2_{2N-1}c'_{\rm pc} + (B_{2N-2}B'_{2N-1} - B_{2N-1}B'_{2N-2}) \\ &= B^2_{2N-1}\sum_{m=1}^{\infty}\frac{w_m}{(\lambda_m - \kappa_n)^2} + \sum_{\ell=0}^{N-1}\mu_0\tau_\ell B^2_{2\ell} > 0.\end{aligned} \tag{E5}$$

Here, the implication from eq. (A8) that

$$B_{2N-2}(\zeta)A_{2N-1}(\zeta) - A_{2N-2}(\zeta)B_{2N-1}(\zeta) = 1 \tag{E6}$$

has been used. Moreover,

$$B_{2N-2}(\zeta)B'_{2N-1}(\zeta) - B'_{2N-2}(\zeta)B_{2N-1}(\zeta) = \sum_{\ell=0}^{N-1}\mu_0\tau_\ell B^2_{2\ell}(\zeta). \tag{E7}$$

If, however, $B_{2N-1}(-\lambda_j) = 0$ for some j, then eq. (E6) yields $A_{2N-1}(-\lambda_j) \neq 0$ and therefore $\lambda_j =: \kappa_n$ will also be a pole of $c(\zeta)$. Then eq. (E1) gives

$$\lim_{\zeta\to-\kappa_n} c_{\rm pc}(\zeta)B_{2N-1}(\zeta) = \lim_{\zeta\to-\kappa_n}\frac{w_j B_{2N-1}(\zeta)}{\zeta + \lambda_j} = -B_{2N-2}(-\kappa_n). \tag{E8}$$

Therefore, eq. (E5) is replaced by

$$1/v_n = B^2_{2N-2}(-\kappa_n)/w_j + \sum_{\ell=0}^{N-1}\mu_0\tau_\ell B^2_{2\ell}(-\kappa_n) > 0. \tag{E9}$$

A detailed analysis provides for $n \gg 1$ the asymptotic results $\kappa_n = \mathcal{O}(n^2)$ and

$$\begin{aligned} d_N > 0: &\quad c_{\rm pc}(-\kappa_n) \to -d_N, &&\quad v_n = \mathcal{O}(\kappa_n^{-2N}), \\ d_N = 0: &\quad c_{\rm pc}(-\kappa_n) \to 1/(\mu_0\tau_{N-1}\kappa_n), &&\quad v_n = \mathcal{O}(\kappa_n^{-2N+1}). \end{aligned} \tag{E10}$$

(ii) $I = \infty$: now $c_{\rm pc}(\zeta)$ has a branch cut from $\zeta = -\lambda_B$ to $\zeta = -\infty$. For $\zeta = -\lambda$, $\lambda < \lambda_B$, the response $c_{\rm pc}(\zeta)$ is also real, see eq. (3.9) or eq. (3.22) for an example. Therefore, in this λ range, the real function $B_{2N}(\zeta)$ may have a number of zeros at $\zeta = -\kappa_n,\ \kappa_n < \lambda_B$. Again, a possible pole λ_m of $c_{\rm pc}(\zeta)$ is suppressed if $B_{2N-1}(-\lambda_m) \neq 0$; otherwise, the pole subsists in $c(\zeta)$ with the residual given by eq. (E9). For $\zeta = -\lambda$, $\lambda > \lambda_B$, the response $c_{\rm pc}$ is complex. From eq. (E1), it follows that now $B_{2N}(\zeta) = 0$ has no solution. Therefore, recalling eqs (1.11) and (E6),

$$w(\lambda) = \frac{w_{\rm pc}(\lambda)\Theta(\lambda - \lambda_B)}{|B_{2N}(-\lambda + i0^+)|^2} + \sum_n v_n \delta(\lambda - \kappa_n),\ \kappa_n < \lambda_B, \tag{E11}$$

where $\Theta(\cdot)$ is again a Heaviside step function. Assuming for $\sigma_{\rm pc}$ the quite general power law (3.18) when approaching $z = z_N$ from below, we have, referring to eq. (3.13), $c_{\rm pc}(\zeta) = \mathcal{O}(1/\zeta^\epsilon)$ for $|\zeta| \to \infty$ and $w_{\rm pc}(\lambda) = \mathcal{O}(1/\lambda^\epsilon)$ for $\lambda \to \infty$, $0 < \epsilon < 1$. With reference to eqs (E1) and (A5), the leading term of B_{2N} for $\lambda \to \infty$ is $\sim [d_N + c_{\rm pc}(-\lambda + i0)]\lambda^N$. Therefore in this limit,

$$\begin{aligned} d_N > 0: &\quad w(\lambda) = \mathcal{O}(\lambda^{-2N-\epsilon}), \\ d_N = 0: &\quad w(\lambda) = \mathcal{O}(\lambda^{-2N+\epsilon}). \end{aligned} \tag{E12}$$

(For the introductory example of Section 3.3 holds $N = 1$, $\epsilon = 1/2$, $d_N = 0$ and $\lambda_B = p$.)

If $d_N > 0$, eqs (E10) and (E12) allow the $2N$ moments s_k, $k = 0, \ldots, 2N - 1$, to be calculated and, if $d_N = 0$, the $2N - 1$ moments s_k, $k = 0, \ldots, 2N - 2$, can be obtained. In both cases, the number of moments agrees with the number of thin-sheet parameters. Therefore, the thin-sheet parameters can be determined from the given moments, which in fact do not depend on $\sigma_{\rm pc}(z)$ (see the introductory example of Section 3.3).